Symmetry and structure of quantized vortices in superfluid ^{3}He-B

M. M. Salomaa
Low Temperature Laboratory, Helsinki University of Technology, SF-02150 Espoo 15, Finland

G. E. Volovik
L. D. Landau Institute for Theoretical Physics, U.S.S.R. Academy of Sciences, 117334 Moscow, U.S.S.R.
(Received 22 June 1984)

We present a symmetry classification for the vortices in superfluid ^{3}He. We find that in superfluid ^{3}He-B there may exist five different singly quantized axially symmetric vortex lines, which are different from each other in their internal discrete symmetries. A phenomenological Landau theory is constructed for all the possible phase transitions between the singly quantized axisymmetric vortices. Our detailed numerical calculations of the vortex core structure in the Ginzburg-Landau regime show that the vortex with minimum free energy, the one that we have identified with the vortex actually observed near T_c in the NMR experiments on rotating ^{3}He-B, possesses a novel new structure: The discrete broken symmetry in this vortex is space parity P; the vortex has a superfluid core with the A phase and a spontaneously ferromagnetic β phase, which is not known to occur in bulk ^{3}He. This core structure explains the measured large magnetic moment of the vortex, and also the orienting effect of the vortices on the ^{3}He-B order parameter in the rotating superfluid through the susceptibility anisotropy. For this superfluid core vortex we find that there exist nodes in the ^{3}He quasiparticle energy gap inside a finite radius from the vortex axis. We define the distance—two to three Ginzburg-Landau coherence lengths—at which the nodes first appear as the core radius of the B-phase vortex. Physical properties of vortices with broken symmetry are discussed: The vortices may display a spontaneous electric polarization and/or a spontaneous axial supercurrent, depending on the symmetry of the vortex core matter.

I. INTRODUCTION

Significant progress has been made during the last two years in the investigation of the quantized vortex lines in the superfluid phases of rotating liquid ^{3}He with use of the NMR technique.[1-3] Several unexpected and fundamentally new intriguing phenomena pertaining to vorticity in anisotropic superfluids have already been discovered in the course of these recent first experiments. In the rotating A phase, extraordinary continuous vortices have been identified.[1,4,5] In contrast with the usual "classical" quantized vortex line in superfluid ^{4}He (He II), which possesses a singularity in the hard core of the vortex (the vortex core in He II has a radius of the order of the superfluid coherence length ξ, where ξ for He II is a few angströms, with the circulating potential flow of the superfluid component around the vortex core axis), these continuous vortices in ^{3}He-A have no singular core of the size of the coherence length ξ (here the coherence length for superfluid ^{3}He is $\xi \cong 10^{-6}$ to 10^{-5} cm). Instead, they exhibit continuous vorticity of superflow, which is concentrated inside the soft core of the vortex, having a radius of the order of several dipole lengths $\xi_D \cong 10^{-3}$ cm, which is hundreds of times larger than ξ.[4,5] This unique behavior of the quantized vortices in ^{3}He-A is a consequence of the peculiar symmetry break in the A phase, namely the broken relative gauge-orbital symmetry, which serves to couple the superfluid and liquid-crystal-like properties of ^{3}He-A.

In the B phase, the gauge symmetry is not coupled intrinsically with the rotational symmetry and the behavior of the vortices in ^{3}He-B was initially expected to be quite similar to that of the classical vortex lines in ^{4}He, with a singular hard core of the size of the coherence length ξ. However, the NMR measurements on vortices in the rotating B liquid have proven that the vortices in ^{3}He-B are much more interesting and that the vortex core structure is quite nontrivial. In particular, experiments have revealed two exotic properties of the vortices in ^{3}He-B, which do not take place for the vortices in superfluid ^{4}He:

(i) A first-order phase transition was found,[6] which was attributed to a change in the vortex core structure at $T=0.6T_c$ (at the pressure $p=29.3$ bars). Recently this phase transition was mapped in the p-T plane.[7]

(ii) The spontaneous magnetic moment of the vortices was discovered.[3]

The vortex magnetization arises due to the specific breaking of the relative spin-orbital rotational symmetry in the B phase. As a consequence, the spin and orbital motions in ^{3}He-B are intrinsically coupled and hence the superflow around the vortex core produces the magnetization,[8] which is concentrated in the vortex core.

Thus the hard vortex core in superfluid ^{3}He-B is quite a nontrivial system: In the experiments, there exist at least two different vortex core structures with different magnitudes of their spontaneous magnetic moments. This highly interesting phase transition of the vortex core structure in superfluid ^{3}He-B, as compared with the usual vortex

line in superfluid ^{4}He, is the outcome of two different factors acting in unison:

(i) The superfluid coherence length ξ in ^{3}He-B is much larger than that in He II, such that a cross section of the core with thickness equal to the interatomic spacing contains 10^5 atoms. Therefore, the hard core of the vortex line in superfluid ^{3}He may be considered as a macroscopic system which may undergo phase transition(s).

(ii) In contrast to the simple order parameter ψ in superfluid ^{4}He, the matrix order parameter $A_{\alpha i}$ in superfluid ^{3}He contains in general 18 real components, which form a reducible representation of a large symmetry group, which includes as symmetry operations the spin and orbital rotations and gauge transformations. This property of the order parameter makes possible the existence of several vortex core structures which possess different internal symmetries.

In analogy with the classification of the superfluid phases in bulk liquid ^{3}He or in other condensed-matter systems, a symmetry analysis allows one to classify the different phases of "vortex core matter." In doing so, we found[8] that in contrast with the single vortex solution possible in ^{4}He or with the usual Abrikosov vortex line in superconductors, there may exist as many as five distinct axially symmetric vortices in superfluid ^{3}He-B. For these different vortex structures we introduced the notation as the o, u, v, w, and uvw vortices. Each of these vortices displays different discrete internal symmetries of vortex core matter. We investigated numerically the relative stability of these vortices near T_c, where the Ginzburg-Landau expansion for the free-energy functional in terms of the order-parameter matrix $A_{\alpha i}$ is applicable. The vortex core structure in the B phase has earlier been considered in this regime by several different authors.[9–11] However, all the axially symmetric vortices that have been considered by these authors either correspond to the so-called o vortex in our classification scheme, or they represent inconsistent *Ansätze* in containing less than the minimal five components of the order-parameter matrix. The o vortex is the most symmetric consistent vortex solution in superfluid ^{3}He-B; it is described by five real functions (pairing amplitudes) of the radial distance from the vortex axis. All these functions vanish on the vortex axis, where the superfluidity is broken, such that the o vortex possesses a normal core. The numerical solution for these five functions was first obtained by Ohmi *et al.*[10] Note that already this most symmetric possible vortex structure in ^{3}He-B is nonunitary, analogously to the nonunitary vortex structures which have normal core that have been discussed for the hypothetical $^3P_2$ pairing of neutrons that has been conjectured by several authors[12] to occur in neutron stars.

We have found, however, that throughout the whole range of values of the strong-coupling parameter δ that are practically relevant for superfluid ^{3}He-B, this most symmetric o vortex is always unstable with respect to the v vortex in which one of the discrete internal symmetries is spontaneously broken. The v vortex contains nine real pairing amplitudes as functions of the radial distance r from the vortex axis. In particular, two of these amplitudes do not vanish on the vortex axis, such that the core of the v vortex does not consist of normal liquid ^{3}He. Instead, these finite Cooper-pairing amplitudes at $r=0$ correspond to two superfluid components in the hard core of the v vortex: One of these is the A phase, while the other is the so-called magnetic β phase, which has spontaneously ferromagnetically ordered spins of the Cooper pairs. The β phase is never stable in the bulk liquid; it may only exist in the ^{3}He-B vortex core. The u vortex with ten amplitudes featuring a normal core, and the w vortex with nine amplitudes and with a superfluid core, which correspond to the other broken discrete symmetries of the o vortex, are energetically unstable towards reduction into the o vortex and hence also to the v vortex.

The further break of the v vortex symmetry is possible; this gives rise to a large variety of phase transitions. The v vortex may, for example, transform either into the least symmetric among the axially symmetric vortices, the so-called uvw vortex with all 18 pairing amplitudes and with a superfluid core structure, or to an axially asymmetric vortex core structure. The study of such possible soft-mode instabilities will require considerable analytic and computing efforts. However, these future investigations will not change the central important result of our present paper: The hard core of the stable vortex in superfluid ^{3}He-B at low pressures consists of superfluid and it contains a new ferromagnetic component which is essentially responsible for the measured[3] large magnetic moment of the vortex. The v vortex core also contains the superfluid A phase, due to which the vortex becomes a nucleation center for the A phase in the metastable bulk B phase, as shown in detail in this paper. Due to the broken parity, the stable v vortex, in addition, displays a spontaneous electric polarization, which is concentrated in the vortex core.

The large variety of the possible phase transitions between all the different axisymmetric singly quantized o, u, v, w, and uvw vortices may be investigated with the aid of a phenomenological Landau theory of phase transitions, which is presently also known widely as "catastrophe theory."[13] The relevant Landau free-energy functional describing the corresponding possible phase transitions is constructed in this paper with the use of the discrete symmetry classification of the vortices. The Landau theory predicts various kinds of phase transitions, both of second and first orders. For example, the transition between the u and v vortices as well as the ones between the different uvw vortices, which may exist according to the Landau theory, are of first order. And note that any of these transitions may be the likely candidate for the observed first-order transition in the vortex-core structure.[6,7]

This paper is organized as follows. In Sec. II we discuss the symmetry of linear defects in condensed matter using as examples the vortices in superfluid ^{4}He and the vortices in ferromagnets with an easy-plane type of an anisotropy. In Sec. III we classify the axisymmetric vortex solutions in the B phase in terms of their discrete internal symmetries and construct the Landau theory of phase transitions for the vortex core structure. In Sec. IV we present our numerical calculations of the vortex core structures for the o, u, v, and w vortices in the Ginzburg-

Landau regime and establish their mutual stability. Section V contrasts the structures of the energy gaps in normal-core and superfluid-core vortices. In Sec. VI the distribution of the B-phase order parameter far from the vortex core is considered. We take into account the dipole forces and the magnetic field term and investigate their influence on the vortex structure and the influence of the vortices on the NMR signal. In Sec. VII the magnetic moment of the vortices is considered.

The unique physical properties of the v and w vortices, with broken symmetry, are discussed in Sec. VIII. It is shown that the parity violation results in a spontaneous electric polarization in the cores of the v and uvw vortices, while the w and uvw vortices possess a spontaneous axial supercurrent.

Multiply quantized vortices in superfluid ^{3}He-B (Refs. 14 and 15) will be discussed in detail elsewhere.[16] An extension of the vortex symmetry classification to the case of the axisymmetric vortices in the rotating A phase[15] and to the vortex lattice in rotating superfluid ^{3}He (Ref. 15) is presented in detail in a companion paper.[17]

II. THE SYMMETRY OF LINEAR DEFECTS IN ORDERED MEDIA

Phase transitions in condensed matter are, as a rule, accompanied with a change in the symmetry of the system. We presume that also the observed phase transition of the vortex core matter in rotating superfluid ^{3}He-B is associated in a similar way with a change in the symmetry of this matter. Therefore, there arises the problem of classifying the states of linear defects (such as vortices) in ordered matter by symmetry groups. This is distinct from the topological classification of linear defects,[18] which divides the defects into different classes, each with a given value of the topological invariant (i.e., the topological charge). Specifically, the symmetry analysis can distinguish the different defects inside the same topological class. This is precisely what we need here, because the vortices in rotating superfluid ^{3}He-B have the same topological charge on either side of the vortex core transition (assuming that both vortices are singly quantized; see Refs. 14, 15, and 16), and are only distinguished by the internal structure of the vortex core.

The general symmetry approach to linear defects is not yet as complete as the topological approach because even for the phases of condensed bulk matter the symmetry classification of different possible states of media has been only partially accomplished. For example, all the possible states of media with spontaneously broken Euclidean symmetry have been completely enumerated:[19] These include crystals with all the 230 (three-dimensional) crystallographic space-group symmetries, predicted in the last century, and different types of liquid crystals. But the question still remains open with regard to superfluid ^{3}He, which appears to be the most complicated condensed-matter system, with several symmetries simultaneously broken: the group $[\mathrm{SO}(3)]^{(L)}$ of space (orbital) rotations, the group $[\mathrm{SO}(3)]^{(S)}$ of spin rotations, the gauge group U(1), and time inversion T. The formation of the vortex lattice in the rotating container in addition breaks the translational symmetry t and space parity P. Due to the large number of simultaneously broken symmetries, the full symmetry classification of all the possible states of superfluid ^{3}He has not yet been completed even without the breaking of translational invariance (the symmetry classification of the so-called inert[20] superconducting states in crystals with cubic symmetry, where all the continuous symmetries are broken, is discussed in Ref. 21).

Thus leaving aside the general symmetry classification of linear defects in condensed matter for the future, we shall here describe several illustrative examples of linear defects in He II and in ferromagnets, their symmetries, and the possibilities of phase transitions in their cores (the symmetry classification of the linear defects, disclinations, in uniaxial and biaxial nematic liquid crystals, is discussed in Ref. 22).

Let us begin by considering the quantized vortex line in superfluid ^{4}He. Here the superfluid order parameter ψ is a complex-valued scalar function. The distribution of the order parameter in the vortex with topological charge m (m denotes the number of circulation quanta of the superfluid velocity around the vortex axis) is represented as

$$\psi(\vec{r})=C(r)e^{im\phi}\,. \tag{2.1}$$

Here r, ϕ, and z are the cylindrical coordinates, with z along the vortex axis. The amplitude of the order parameter obeys $C(r=0)=0$, in order to escape the infinite energy of superflow. Hence superfluidity is broken in the ^{4}He vortex on the vortex axis and the core of the ^{4}He vortex is normal.

Let us find the symmetry group of the state (2.1) which is the subgroup of the general group G of physical laws. The relevant group G for ^{4}He

$$G=[\mathrm{SO}(3)]^{(L)}\times\mathrm{U}(1)\times T\times P\times t \tag{2.2}$$

does not include spin rotations because the ^{4}He atom is spinless. Which part of this group is conserved in the vortex state (2.1)? First of all, clearly the translations t_z along the vortex axis: The vortex state does not change under this transformation since $\hat{p}_z\psi=0$, where $\hat{p}_z=(\hbar/i)\partial/\partial z$ is the generator of translations along z.

The ^{4}He vortex state (2.1) is not invariant, however, either under a rotation (even a rotation about the vortex axis z through the angle ϕ_0 changes the order parameter as follows: $\psi\rightarrow\psi e^{im\phi_0}$) or under a gauge transformation, which also corresponds to a change of the phase factor. However, note that a definite combined rotation and gauge transformation does not change the state (2.1). The generator of this combined symmetry group is

$$\hat{Q}=\hat{L}_z-m\hat{I}\,, \tag{2.3}$$

where

$$\hat{L}_z=\frac{1}{i}\frac{\partial}{\partial\phi}$$

is the generator of rotations about z, and $\hat{I}$ denotes the generator of gauge transformations, which has the following action on ψ: $\hat{I}\psi=\psi$, $\hat{I}\psi^*=-\psi^*$. It is easy to verify that the state (2.1) obeys

$$\hat{Q}\psi=\frac{1}{i}\frac{\partial}{\partial\phi}\psi-m\psi=0\,. \tag{2.4}$$

In what follows, we shall refer to the symmetry described by the generator $\hat{Q}$ as axial, because all the physical properties of a state with the eigenvalue $Q=0$ are axially symmetric. For example, let us consider the superfluid velocity

$$\vec{v}_s=\frac{\hbar}{2m_4 i}\frac{\psi^*\vec{\nabla}\psi-\psi\vec{\nabla}\psi^*}{|\psi|^2} . \tag{2.5}$$

Because $\vec{v}_s$ is not transformed by global gauge ($\hat{I}\vec{v}_s=\vec{0}$), the equation $\hat{Q}\vec{v}_s=\vec{0}$ at once implies $\hat{L}_z\vec{v}_s=\vec{0}$, which means axial symmetry.

In the same way, space parity P and time inversion T are not elements of the subgroup H of the vortex state since $T\psi=\psi^*\neq\psi$ and $P\psi(\vec{r})=\psi(-\vec{r})=\psi(r,\phi+\pi)\neq\psi(r,\phi)=\psi(\vec{r})$ for odd m. However, they do conserve the vortex state after being combined with the appropriate other elements of the group G. In particular, applications of the following combinations of the group elements,

$$P_1=PO^{(L)}_{z,m\pi} \text{ and } P_2=TO^{(L)}_{x,\pi} , \tag{2.6}$$

leave the order parameter invariant: $P_1\psi=P_2\psi=\psi$. Above, $O^{(L)}_{z,\theta}$ and $O^{(L)}_{x,\theta}$ denote rotations through the angle θ about the axes z and x, respectively, where x is the axis with respect to which the azimuthal angle ϕ is measured (note that all the physical properties are still invariant under P, e.g., $P\vec{v}_s=\vec{v}_s$).

Hence the symmetry group H of the vortex state (2.1) contains two different continuous groups with the corresponding generators $\hat{p}_z$ and $\hat{Q}=\hat{L}_z-m\hat{I}$, and the two discrete groups P_1 and P_2.

It is important to recognize here that the *Ansatz* (2.1) is the only solution of the equations $\hat{p}_z\psi=0$ and $\hat{Q}\psi=0$. This means therefore that there is only a single type of an axially symmetric vortex with m quanta of circulation. Thus one cannot expect any phase transitions for the ^{4}He vortex, unless the axial symmetry is broken. As we shall see in detail below, the axially symmetric vortex structures are much richer in superfluid ^{3}He, where because of its multicomponent order-parameter tensor one may in fact encounter several possible phase transitions due to the breaking of the corresponding discrete internal symmetries without a break of the axial symmetry.

Another illustrative example is provided by the linear defects in ferromagnets with an easy plane of anisotropy. The order parameter here is the magnetization vector $\vec{M}$, which far from the defect lies in the easy plane. The linear defect in this system is analogous to the vortex line in superfluid ^{4}He.

The asymptotic behavior of such a "vortex" possessing topological charge m and with its axis z perpendicular to the easy plane is

$$\vec{M}=M_0[\hat{x}\cos(m\phi)+\hat{y}\sin(m\phi)] . \tag{2.7}$$

However, the symmetry subgroup H of the relevant group

$$G=[\mathrm{SO}(3)]^{(L)}\times[\mathrm{SO}(3)]^{(S)}\times T\times P\times t \tag{2.8}$$

is larger than for the vortices in superfluid ^{4}He. The continuous symmetry groups of H are just the same: translations t_z along the vortex axis, and the combined symmetry group is

$$\hat{Q}=\hat{L}_z+m\hat{S}_z , \tag{2.9}$$

where instead of the gauge generator $\hat{I}$; there now appears the generator of spin rotations $\hat{S}_z$ ($\hat{S}_z\vec{M}=i\hbar\hat{z}\times\vec{M}$). All the difference is in the discrete subgroup, which contains the elements

$$TO^{(S)}_{z,\pi},\ O^{(J)}_{x,\pi}, \text{ and } PO^{(L)}_{z,m\pi} , \tag{2.10}$$

and their combinations (here $T\vec{M}=-\vec{M}$ is time inversion, $O^{(S)}_{z,\pi}$ is a rotation of the spin space by π about z, and $O^{(J)}_{x,\pi}=O^{(S)}_{x,\pi}O^{(L)}_{x,\pi}$ denotes the rotations of the spin and orbital coordinate spaces by π about x one after another). The addition of the new subgroup as well as increasing the dimension of the representation (three components of $\vec{M}$ instead of the two components of ψ) serve to produce the possibility of different vortex core structures.

The subgroup H, generated by $\hat{S}_z$, $\hat{Q}$, and by the discrete elements (2.10), is the symmetry group of the asymptotics (2.7) and is therefore the maximal one of the possible symmetry groups of the "vortex." The solution corresponding to the maximal symmetry group always exists, which reflects a fundamental mathematical theorem. The solution is

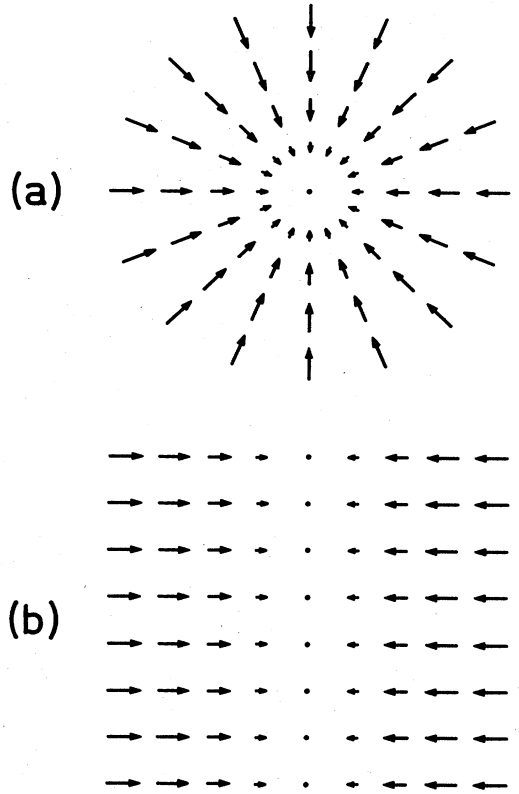

FIG. 1. Schematic illustration of the maximally symmetric linear defect in a ferromagnet with an easy plane of anisotropy, Eq. (2.11), where the order parameter vanishes on the vortex axis: $\vec{M}(\vec{r}=\vec{0})=\vec{0}$. Here the arrows represent the projections of the magnetization vector $\vec{M}(\vec{r})$ in two different planes as follows: (a) A cross section in a plane perpendicular to the axis of the linear defect; (b) the distribution of magnetization in a plane containing the axis of the linear defect.

$$\vec{M}=M(r)[\hat{x}\cos(m\phi)+\hat{y}\sin(m\phi)]\ , \tag{2.11}$$

with $M(r=0)=0$ in order to prevent the divergence in the energy in the core. This vortex state is illustrated in Fig. 1.

However, it is more advantageous to break one of the discrete symmetries, because this allows for $\vec{M}$ not to equal zero at the core, but to escape into the third dimension; see Fig. 2. We therefore write

$$\vec{M}=M_{\perp}(r)[\hat{x}\cos(m\phi)+\hat{y}\sin(m\phi)]+M_{\parallel}(r)\hat{z}\ . \tag{2.12}$$

This form conserves the continuous symmetry but some of the discrete symmetries are now broken; instead of (2.10) one has now reduced the number of the discrete symmetry elements:

$$PO^{(L)}_{z,m\pi} \quad \text{and} \quad TO^{(S)}_{z,\pi}O^{(J)}_{x,\pi}=TO^{(S)}_{y,\pi}O^{(L)}_{x,\pi}\ . \tag{2.13}$$

A new degeneracy arises due to breaking of the discrete symmetry: The states with positive and negative $M_{\parallel}(r)$ in the core have equal energies. That is, the vortex core is characterized by a new quantum number—the direction of the magnetization at the vortex axis.[23]

Thus the discrete symmetry gives rise to the different vortex structures, (2.11) and (2.12), with different symmetries of the vortex core. Therefore, one may expect to find a second-order transition from the structure (2.11) to (2.12) with the breaking of a discrete symmetry but without breaking of axial symmetry.

An even more interesting situation occurs in the case of vortices in superfluid ^{3}He, where there is also the possibility for the existence of first-order transitions in addition to second-order transitions in the vortex core structure.

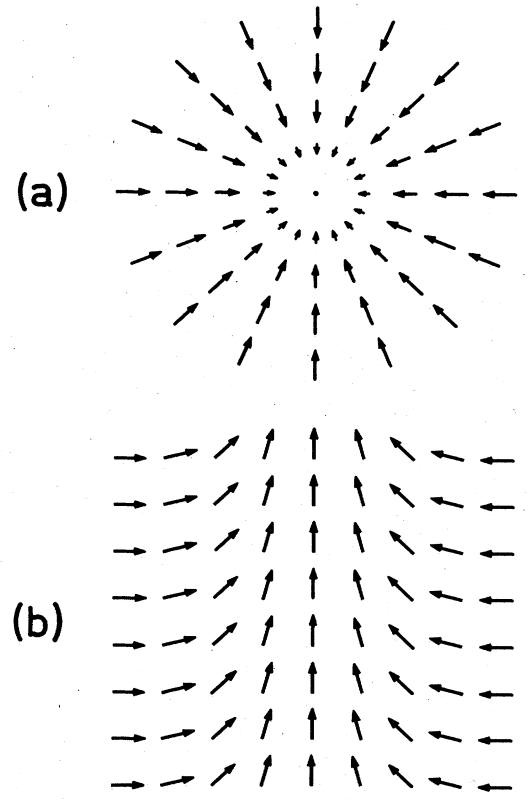

FIG. 2. Linear defect with a broken discrete symmetry, represented by Eq. (2.12), in a ferromagnet with an easy plane of anisotropy. (a) The cross-sectional projection coincides with that in Fig. 1(a). (b) The order parameter $\vec{M}(\vec{r})$ remains finite on the axis of the vortex line through an escape into the third dimension.

III. SYMMETRY CLASSIFICATION OF THE VORTICES IN ^{3}He-B

The general group G of physical laws, which is broken in superfluid ^{3}He, is

$$G=[\mathrm{SO}(3)]^{(L)}\times[\mathrm{SO}(3)]^{(S)}\times\mathrm{U}(1)\times T\times P\times t\ . \tag{3.1}$$

The order parameter in superfluid ^{3}He, which provides the realization of a representation of this group, is the complex 3×3 matrix $A_{\alpha i}$, with the spin (α) and orbital (i) indices. This matrix transforms under the action of the various elements of the group (3.1) in the following ways:

$$\hat{L}_k A_{\alpha i}=(\hat{L}^{\mathrm{ext}}_k+\hat{L}^{\mathrm{int}}_k)A_{\alpha i}$$
$$=\frac{1}{i}e_{kmn}r_m\frac{\partial}{\partial r_n}A_{\alpha i}-ie_{kil}A_{\alpha l}\ , \tag{3.2a}$$

$$\hat{S}_\beta A_{\alpha i}=-ie_{\beta\alpha\gamma}A_{\gamma i}\ . \tag{3.2b}$$

$$U_\theta=e^{i\hat{I}\theta},\quad \hat{I}A_{\alpha i}=A_{\alpha i},\quad \hat{I}A^*_{\alpha i}=-A^*_{\alpha i}\ , \tag{3.2c}$$

$$PA_{\alpha i}(\vec{r})=-A_{\alpha i}(-\vec{r})\ , \tag{3.2d}$$

$$TA_{\alpha i}=A^*_{\alpha i},\quad t_{\vec{r}_0}A_{\alpha i}=A_{\alpha i}(\vec{r}-\vec{r}_0)\ . \tag{3.2e}$$

Here $\hat{L}$ is the generator of rotations in the orbital space, including the external $\hat{L}^{\mathrm{ext}}$ and internal $\hat{L}^{\mathrm{int}}$ parts, the latter transforming $A_{\alpha i}$ as a vector in the orbital index; $\hat{S}$ is the generator of spin rotations; U_θ is the gauge transformation through the phase θ; the minus sign as a prefactor of $A_{\alpha i}$ in the parity transformation P reflects the vector representation of the order parameter in the coordinate space.

In the uniform bulk B phase, the matrix $A_{\alpha i}$ reduces to the arbitrary orthogonal matrix $R_{\alpha i}$:

$$A_{\alpha i}=\Delta(T)R_{\alpha i}e^{i\Phi}\ , \tag{3.3}$$

where Φ is the phase factor and $\Delta(T)$ denotes the temperature-dependent scalar amplitude of the order parameter (energy gap). The continuous and discrete elements of the symmetry group H of this state are

$$[\mathrm{SO}(3)]^{(\tilde{J})},\quad U_\Phi TU_{-\Phi},\quad PU_\pi,\quad t\ , \tag{3.4}$$

where $[\mathrm{SO}(3)]^{(\tilde{J})}$ is the combined spin and space rotation, generated by

$$\hat{\tilde{J}}_i=\hat{L}_i+R_{\alpha i}\hat{S}_\alpha\ . \tag{3.5}$$

Vortices in the B phase, like the classical quantized vortices in He II, are quantized with an integer number of circulation quanta in superfluid ^{3}He:

$$\kappa_3=\frac{h}{2m_3}\cong0.6616\times10^{-3}\ \mathrm{cm}^2/\mathrm{sec}\ . \tag{3.6}$$

Note that the circulation quantum in superfluid ^{3}He differs from that in superfluid ^{4}He, $\kappa_4 = h/m_4 \cong 0.9970 \times 10^{-3}$ cm^2/sec, not only in the occurrence of the different isotopic mass in Eq. (3.6), but also through the extra factor of 2, which is due to the Cooper pairing. Far from the vortex axis the order parameter in ^{3}He-B imitates the behavior of a He II vortex:

$$A_{\alpha i}(r \to \infty) = \Delta(T) R_{\alpha i} e^{im\phi} . \tag{3.7}$$

From this asymptotic form alone, one may already deduce the maximal symmetry group of the vortex state in the rotating B phase of superfluid ^{3}He.

It is important to note the simplification that for a vortex line in ^{3}He-B, we may consider the spin and orbital rotations independently. This is because the size of the vortex core with its structure on distances of the order of ξ is much less than the dipole length $\xi_D \cong 10^{-3}$ cm. Therefore, the spin-orbital (dipole) interaction does not influence the structure of the hard core of the vortex, and it may be neglected. In this situation the symmetry of the asymptotics is defined by the following generators of continuous transformations and elements of discrete symmetries:

$$\hat{p}_z, \quad \hat{Q} = \hat{\vec{J}}_z - m\hat{I}, \quad P_1 = PU_{(m+1)\pi} , \quad P_3 = TO^{(\vec{J})}_{x,\pi} . \tag{3.8}$$

In order to avoid needing to consider the matrix $R_{\alpha i}$ in what follows, one may use the simpler coordinate axes for the spin system, which are rotated by the matrix $R_{\alpha i}$ itself with respect to the laboratory coordinate frame. The rotation matrix reduces in these coordinates into $R_{\alpha i} = \delta_{\alpha i}$, the asymptotics are given by

$$A_{\alpha i}(r \to \infty) = \Delta(T) \delta_{\alpha i} e^{im\phi} , \tag{3.9}$$

and the operator $\hat{\vec{J}}$ transforms into the operator of the total angular momentum, i.e.,

$$\hat{\vec{J}} \to \hat{\vec{J}} = \hat{\vec{L}} + \hat{\vec{S}} .$$

In analogy with our examples of vortices in ^{4}He and in magnets, the symmetry $\hat{Q}$ here means the axial symmetry of the vortex in ^{3}He-B. In order to find the general representation for the axially symmetric vortex state, one must solve the equation

$$\hat{Q} A_{\alpha i} = 0 . \tag{3.10}$$

For this purpose let us decompose $A_{\alpha i}$ in terms of the eigenfunctions $e^{in\phi}$, λ_i^ν, and λ_α^μ of the operators $\hat{L}_z^{\text{ext}}$, $\hat{L}_z^{\text{int}}$, and $\hat{S}_z$:

$$A_{\alpha i} = \Delta(T) \sum_{\mu,\nu,n} C_{\mu\nu n}(r) \lambda_\alpha^\mu \lambda_i^\nu e^{in\phi} , \tag{3.11}$$

with

$$\hat{L}_z^{\text{int}} \lambda_i^\nu = \nu \lambda_i^\nu , \quad \lambda_i^\pm = \frac{1}{\sqrt{2}} (\hat{x}_i \pm i\hat{y}_i) , \quad \lambda_i^0 = \hat{z}_i , \tag{3.12}$$

$$\hat{S}_z \lambda_\alpha^\mu = \mu \lambda_\alpha^\mu , \quad \lambda_\alpha^\pm = \frac{1}{\sqrt{2}} (\hat{x}_\alpha \pm i\hat{y}_\alpha) , \quad \lambda_\alpha^0 = \hat{z}_\alpha . \tag{3.13}$$

Here $(\hat{x}_i, \hat{y}_i, \hat{z}_i)$ and $(\hat{x}_\alpha, \hat{y}_\alpha, \hat{z}_\alpha)$ are unit vectors in the orbital laboratory frame and the spin frame, which are rotated by the matrix $\underline{R}$ with respect to each other, i.e., $\lambda_\alpha^\mu = R_{\alpha i} \lambda_i^\mu$, and the eigenvalues μ and ν of the projections of the Cooper-pair spin and orbital momenta in Eqs. (3.12) and (3.13) may assume the values 0 and ± 1. The expression (3.11) obeys the condition of axial symmetry, $\hat{Q} A_{\alpha i} = 0$, provided that the quantum numbers n, μ, and ν satisfy $n = m - \mu - \nu$. Therefore, the most general expression for an axially symmetric vortex state

$$A_{\alpha i} = \Delta(T) \sum_{\mu,\nu} C_{\mu\nu}(r) \lambda_\alpha^\mu \lambda_i^\nu e^{i(m-\mu-\nu)\phi} , \tag{3.14}$$

with

$$\lambda_\alpha^\mu = R_{\alpha i} \lambda_i^\mu , \tag{3.15}$$

contains in general the nine complex-valued amplitudes $C_{\mu\nu}(r)$ as functions of the radial distance r from the vortex axis.

Each function $C_{\mu\nu}$ describes the amplitude of Cooper pairing of the ^{3}He atoms into a respective general p-wave superfluid state, characterized by the quantum numbers μ and ν, referring to the projections of the Cooper-pair spin and orbital momenta onto the respective coordinate spaces, spanned by the vectors λ_α^μ and λ_i^ν. For example, $C_{0+}(r)$, with the projections $\mu = 0$ and $\nu = +1$ of pair spin and orbital momenta, represents the A-phase Cooper-pairing amplitude.

However, the number of the pairing amplitudes $C_{\mu\nu}(r)$ is reduced if one considers the most symmetric possible vortex solution, which possesses the symmetry of the asymptotics, Eqs. (3.8), including the discrete symmetry elements P_1 and P_3. The latter form the group $\mathbb{Z}_2 \times \mathbb{Z}_2$, which contains the following four elements:

$$1 , \tag{3.16a}$$

$$P_1 = PU_{(m+1)\pi} \quad (P_1^2 = 1) , \tag{3.16b}$$

$$P_3 = TO^{(J)}_{x,\pi} \quad (P_3^2 = 1) , \tag{3.16c}$$

$$P_2 = P_1 P_3 \quad (P_2^2 = 1) . \tag{3.16d}$$

Under these different discrete symmetry transformations, the pairing amplitudes $C_{\mu\nu}$ obey the following relations:

$$\hat{P}_1 C_{\mu\nu} = (-1)^{\mu+\nu} C_{\mu\nu} , \tag{3.17}$$

$$\hat{P}_2 C_{\mu\nu} = C^*_{\mu\nu} , \tag{3.18}$$

and

$$\hat{P}_3 C_{\mu\nu} = (-1)^{\mu+\nu} C^*_{\mu\nu} . \tag{3.19}$$

The most symmetric vortex, the o vortex, which possesses the maximal discrete symmetry

$$\hat{P}_1 C_{\mu\nu} = \hat{P}_2 C_{\mu\nu} = \hat{P}_3 C_{\mu\nu} = C_{\mu\nu} , \tag{3.20}$$

has only five nonvanishing real amplitudes, C_{++}, C_{+-}, C_{00}, C_{-+}, and C_{--}. It is important to recognize that all these five amplitudes also necessarily must enter the expressions due to their mutual nonlinear coupling in the Gor'kov equations (or in the Ginzburg-Landau equations for temperatures near T_c). The number of the pairing amplitudes could only be reduced from this due to an accidental (but improbable) hidden symmetry in these equa-

tions. This means that the *ad hoc* one-parameter vortex *Ansatz*,

$$A_{\alpha i}=\Delta(T)C(r)\delta_{\alpha i}e^{im\phi}\ , \tag{3.21}$$

which would imitate the vortex state in superfluid ^{4}He, corresponds to the completely arbitrary additional constraints $C_{++}=C_{--}=0$ and $C_{+-}=C_{00}=C_{-+}=C$. The *Ansatz* (3.21) is therefore not at all a solution of the Gor'kov equations, and neither is the vortex *Ansatz* of Passvogel, Schopohl, and Tewordt,[9] with just three nonzero amplitudes. The most symmetric vortex with $m=1$ and with the five real amplitudes was first discussed by Ohmi, Tsuneto, and Fujita.[10] This vortex state with $m=1$ possesses a normal core (however, the most symmetric doubly quantized vortex has a superfluid core, such as all the doubly quantized axisymmetric vortices in ^{3}He-B; see Refs. 14–16): Superfluidity is broken on the vortex axis, where all the five real amplitudes $C_{\mu\nu}$ vanish because their phases

$$\Phi_{\mu\nu}=(1-\mu-\nu)\phi \tag{3.22}$$

have a discontinuity on the vortex axis ($\Phi_{+-}=\Phi_{00}=\Phi_{-+}=-\Phi_{++}=\frac{1}{3}\Phi_{--}=\phi$).

Here, just like for the "vortices" in magnets, one may expect that it is more advantageous to break one of the discrete symmetries in Eqs. (3.16). The discrete vortex symmetry may be broken in three inequivalent ways, depending on which symmetry is retained, P_1, P_2, or P_3. We denote the corresponding vortices with these broken symmetries as the u, v, and w vortices; see Table I:

(i) The u vortex, with the discrete symmetry P_1, contains the same five amplitudes $C_{\mu\nu}=(-1)^{\mu+\nu}C_{\mu\nu}$ as the o vortex, but now these amplitudes are complex valued; they vanish at the center of this vortex, which has a normal core.

(ii) The v vortex, with the symmetry P_2, contains the nine real amplitudes $C_{\mu\nu}=C^*_{\mu\nu}$; that is, the amplitudes C_{+0}, C_{0+}, C_{0-}, and C_{-0} in addition to those five in the o vortex. In particular, two among these four additional pairing amplitudes, C_{+0} and C_{0+}, need not vanish at $r=0$, since their phases $\Phi_{+0}=\Phi_{0+}=0$ display no discontinuity on the vortex axis. These superfluid components in the vortex core describe the A phase (C_{0+}) and the ferromagnetic superfluid β phase (C_{+0}), with its magnetic moment directed along the axis $\hat{z}_\alpha$ in the rotated spin frame, i.e., along $R_{\alpha i}\hat{z}_i$ in the laboratory coordinates.

(iii) The w vortex with the discrete symmetry P_3 also contains nine amplitudes, which obey $C_{\mu\nu}=(-1)^{\mu+\nu}C^*_{\mu\nu}$. Five of the amplitudes are real (the same ones that occur in the o vortex), while the four additional ones are purely imaginary; these describe the same additional Cooper-pairing states as in the v vortex.

Each of these three vortices is degenerate due to the appropriate broken symmetry: A change in the sign of the additional components does not change the energy of the vortex, because this is a symmetry operation.

The breaking of the discrete vortex symmetries is now described using the phenomenological Landau theory of phase transitions, with real order parameters. In our present case, with three elements of discrete symmetries, one must introduce three real parameters u, v, and w, each associated with the respective broken symmetry. The parameter u here represents simultaneously the mutual amplitude of all the five additional imaginary components that are present in the u vortex, v refers correspondingly to the four additional real amplitudes of the v vortex, and w describes the four additional imaginary amplitudes present in the w vortex. The symmetry properties of these amplitudes are as follows:

$$P_1u=u,\quad P_2u=-u,\quad P_3u=-u\ , \tag{3.23a}$$

$$P_2v=v,\quad P_3v=-v,\quad P_1v=-v\ , \tag{3.23b}$$

$$P_3w=w,\quad P_1w=-w,\quad P_2w=-w\ . \tag{3.23c}$$

Using these parity properties, we may construct the Landau free-energy functional in terms of the parameters u, v, and w, which must be invariant under the P_1, P_2, and P_3 transformations:

$$F=-au^2-bv^2-cw^2+\tfrac{1}{2}(u^4+v^4+w^4)+euvw+fu^2v^2+gu^2w^2+hv^2w^2\ . \tag{3.24}$$

Note, in particular, that the symmetries (3.23) admit the existence of a third-order term in the expression (3.24) for F with the coefficient e.

Depending on the actual values of the phenomenologically introduced coefficients a, b, c, e, f, g, and h, which in general are functions of temperature, pressure, and the external applied magnetic field, Eq. (3.24) may exhibit several different minima. The investigation of the appearance of new minima under a change of external conditions (the investigation of phase transitions in the ^{3}He-B vortex

TABLE I. Group-theoretical symmetry classification of the axisymmetric quantized vortex lines in superfluid ^{3}He-B. For singly quantized vortices ($m=1$) the core fluid can be normal (N) or superfluid (consisting of the superfluid A phase and the ferromagnetic superfluid β phase). For doubly quantized vortices the core is always of superfluid A_1 phase (Refs. 14 and 15), while for vortex lines with three or more quanta of circulation the core matter is normal liquid ^{3}He. Multiply quantized vortices in superfluid ^{3}He-B, first introduced in Ref. 14, are discussed in detail in Refs. 15 and 16.

Vortex	Discrete symmetry	$C_{\mu\nu}$ with $\mu+\nu$ even	$C_{\mu\nu}$ with $\mu+\nu$ odd	States of vortex core matter $m=1$	$m=2$	$m\geq 3$
o	P_1,P_2,P_3	real	zero	N	A_1	N
u	P_1	complex	zero	N	A_1	N
v	P_2	real	real	A and β	A_1	N
w	P_3	real	imaginary	A and β	A_1	N
uvw	none	complex	complex	A and β	A_1	N

core in the present context) is the subject of catastrophe theory.[13] The full catastrophe theory of all the possible phase transitions for this complicated system with the codimension 3 (three external parameters: temperature, pressure, and magnetic field) and with three independent variables is presently under investigation. However, several results may be readily obtained at once on inspection.

The extrema of Eq. (3.24) are obtained as the roots of a system of three coupled algebraic equations of the third order. Thus the number of real solutions is not more than $3^3=27$. According to the Morse theorem, the number of local minima of Eq. (3.24) among these extrema cannot exceed 14. The extrema of F in Eq. (3.24), including the minima, are degenerate according to the broken symmetry. The most symmetric solution, which is invariant under the P_1, P_2, and P_3 transformations: $u=0$, $v=0$, $w=0$ corresponds to the o vortex and is not degenerate. The u vortex with the symmetry P_1 ($u\neq 0$, $v=w=0$) has twofold degeneracy because the P_2 and P_3 transformations change the sign of u according to (3.23), but do not change F in Eq. (3.24). The same holds for the v vortex ($v\neq 0$, $u=w=0$) with the symmetry P_2 and for the w vortex ($w\neq 0$, $u=v=0$) with the discrete symmetry P_3.

Hence the o, u, v, and w vortices may produce seven ($7=1+2\times 3$) real extrema and therefore altogether 20 ($20=27-7$) extrema may correspond to the least symmetric vortices, which we denote as the uvw vortices, because all the parameters u, v, and w are nonzero in these cases. Since each of the discrete symmetries is broken for these uvw vortices, they are fourfold degenerate in accordance with the number of elements in the discrete group of Eq. (3.16). Therefore, there may exist five ($5=20/4$) different possible least symmetric vortices as the extremal solutions of F; however, no more than three of them may correspond to the local minima. Examples of the different uvw vortices may be readily obtained explicitly, provided that one assumes the coefficient e in Eq. (3.24) is small. In this case there may exist three different solutions for the least symmetric vortices, which may be denoted as the uv vortex [$u\neq 0, v\neq 0, w=O(e)$], the vw vortex [$v\neq 0, w\neq 0, u=O(e)$], and the wu vortex [$w\neq 0, u\neq 0, v=O(e)$].

Thus the resulting vortex phase diagram may be quite complicated: besides the second-order transitions $o\rightarrow u, o\rightarrow v, o\rightarrow w$, $u\rightarrow uvw$, $v\rightarrow uvw$, $w\rightarrow uvw$, and $o\rightarrow uvw$, which are associated with broken symmetry, there may occur first-order transitions between the states with different broken symmetries: $u\rightarrow v$, $v\rightarrow w$, $w\rightarrow u$, and first-order transitions between the different least symmetric vortices $uvw\rightarrow uvw$.

In concluding this section we note that (i) we have not considered all the possible linear defects in superfluid ^{3}He-B, but only axisymmetric quantized vortex lines, and (ii) to find the maximal symmetry of the vortices we employed the asymptotics of the order parameter far from the vortex core. In general, in order to find all the symmetry classes of linear defects in condensed matter one needs only to use the asymptotics and vice versa: These classes and their asymptotics may be found on using general symmetry analysis. In particular, one may show that for ^{3}He-B the generator $\hat{Q}$ of the axial symmetry may contain one additional integer quantum number besides m:

$$\hat{Q}=\hat{J}_z-m\hat{I}-p\hat{S}_z \ . \tag{3.25}$$

While m, the number of circulation quanta at infinity, means the index of the vortex, the new integer p may be interpreted as the index of disclination. The axisymmetric vortex representation with two integer indices becomes

$$A_{\alpha i}=\Delta(T)\sum_{\mu,\nu}C_{\mu\nu}(r)\lambda^{\mu}_{\alpha}\lambda^{\nu}_{i}e^{i(m-\nu-\mu+p\mu)\phi} \ . \tag{3.26}$$

For the A phase, m and p may be half-integers (with $m+p$ an integer); this describes the vortices with half-integer numbers of circulation quanta.[24]

IV. VORTEX CORE STRUCTURE IN THE GINZBURG-LANDAU REGIME

In order to find the structures of the o, u, v, w, and uvw vortices and in order to identify them with the vortices observed in the experiments, one must solve the Gor'kov equations subjected to the given symmetries. This appears to be considerably tedious, on account of the fact that the number of components of the order parameter is not less than five. The situation is much simpler near T_c, where one may minimize the Ginzburg-Landau free-energy functional to find the most stable vortex and the possible metastable ones.

The Ginzburg-Landau functional contains, first of all, the bulk (condensation) energy (see, for example, Refs. 25):

$$\begin{aligned}F_B=&-\alpha A^*_{\alpha i}A_{\alpha i}+\beta_1 A^*_{\alpha i}A^*_{\alpha i}A_{\beta j}A_{\beta j}+\beta_2 A^*_{\alpha i}A_{\alpha i}A^*_{\beta j}A_{\beta j}\\&+\beta_3 A^*_{\alpha i}A^*_{\beta i}A_{\alpha j}A_{\beta j}+\beta_4 A^*_{\alpha i}A_{\beta i}A^*_{\beta j}A_{\alpha j}\\&+\beta_5 A^*_{\alpha i}A_{\beta i}A_{\beta j}A^*_{\alpha j} \ ,\end{aligned} \tag{4.1}$$

where $\alpha=N(0)(1-T/T_c)/3$ with $N(0)=m^*k_F/2\pi^2\hbar^2$ denoting the density of the ^{3}He states for one spin projection at the Fermi surface, and the coefficients β_i of the fourth-order invariants are in the weak-coupling approximation given by

$$-2\beta_1=\beta_2=\beta_3=\beta_4=-\beta_5 \ , \tag{4.2}$$

with

$$-\beta_1\equiv\beta_0=\frac{7N(0)\zeta(3)}{240(\pi T)^2} \ .$$

The pressure dependence of the β_i (the "strong-coupling" corrections) are described in terms of the spin-fluctuation (paramagnon) parameter δ:[26]

$$\begin{aligned}&\beta_1=-(1-0.1\delta)\beta_0, \ \ \beta_2=(2+0.2\delta)\beta_0 \ ,\\&\beta_3=(2-0.05\delta)\beta_0, \ \ \beta_4=(2-0.55\delta)\beta_0 \ ,\\&\beta_5=-(2+0.7\delta)\beta_0 \ .\end{aligned} \tag{4.3}$$

The gradient energy in the Ginzburg-Landau functional is given by

$$F_G = K_1 \partial_i A_{\alpha j} \partial_i A^*_{\alpha j} + K_2 \partial_i A_{\alpha i} \partial_j A^*_{\alpha j} + K_3 \partial_i A_{\alpha j} \partial_j A^*_{\alpha i} , \tag{4.4}$$

where for weak coupling

$$K_1 = K_2 = K_3 = K = 7\zeta(3) N(0) \frac{v_F^2}{240(\pi T)^2} . \tag{4.5}$$

For the sake of convenience, we shall normalize the order-parameter components $A_{\alpha i}$ in terms of the bulk equilibrium value:

$$\Delta = \left[\frac{\alpha}{2(3\beta_{12} + \beta_{345})} \right]^{1/2} , \tag{4.6a}$$

$$A_{\alpha i} = \Delta \tilde{A}_{\alpha i} , \tag{4.6b}$$

such that the asymptotics is $\tilde{A}_{\alpha i}(\infty) = R_{\alpha i}$, the energy is in terms of $\alpha\Delta^2$, and distances are measured in units of ξ_{GL}, the temperature-dependent Ginzburg-Landau coherence length: $\vec{r} = \tilde{r}\xi_{GL}$, with

$$\xi_{GL} = \left[\frac{K}{\alpha} \right]^{1/2} = (\tfrac{3}{5})^{1/2} \xi_0 \left[1 - \frac{T}{T_c} \right]^{-1/2} . \tag{4.7}$$

Hence we shall minimize the following expression:

$$\tilde{F} = \int \frac{d^2\tilde{r}}{2\pi} \left[-\tilde{A}^*_{\alpha i} \tilde{A}_{\alpha i} + \tilde{\beta}_1 \tilde{A}^*_{\alpha i} \tilde{A}^*_{\alpha i} \tilde{A}_{\beta j} \tilde{A}_{\beta j} + \tilde{\beta}_2 \tilde{A}^*_{\alpha i} \tilde{A}_{\alpha i} \tilde{A}^*_{\beta j} \tilde{A}_{\beta j} + \tilde{\beta}_3 \tilde{A}^*_{\alpha i} \tilde{A}^*_{\beta i} \tilde{A}_{\alpha j} \tilde{A}_{\beta j} + \tilde{\beta}_4 \tilde{A}^*_{\alpha i} \tilde{A}_{\beta i} \tilde{A}^*_{\beta j} \tilde{A}_{\alpha j} + \tilde{\beta}_5 \tilde{A}^*_{\alpha i} \tilde{A}_{\beta i} \tilde{A}_{\beta j} \tilde{A}^*_{\alpha j} + (\tilde{\partial}_i \tilde{A}_{\alpha j} \tilde{\partial}_i \tilde{A}^*_{\alpha j} + \tilde{\partial}_i \tilde{A}_{\alpha i} \tilde{\partial}_j \tilde{A}^*_{\alpha j} + \tilde{\partial}_i \tilde{A}_{\alpha j} \tilde{\partial}_j \tilde{A}^*_{\alpha i}) + \frac{3}{2} - \frac{5m^2}{\tilde{r}^2 + r_0^2} \right] , \tag{4.8}$$

where the $\tilde{\beta}_i$ are defined as

$$\tilde{\beta}_i = \frac{\beta_i}{2(\beta_{345} + 3\beta_{12})} , \tag{4.9}$$

and the terms $\frac{3}{2}$ and $-5m^2/(\tilde{r}^2 + r_0^2)$ were inserted to subtract out the infinite bulk energy and to compensate for the logarithmically divergent energy of the vortex with m quanta of circulation. We have chosen the parameter r_0 to be 5. The energy of the vortex with m circulation quanta can be expressed in terms of $\tilde{F}$ as follows:

$$F_{\text{vortex}} = \pi\rho_s \left[\frac{\hbar}{2m_3} \right]^2 m^2 \left[\ln \left[\frac{R}{\xi_{GL}} \right] + \frac{1}{5m^2} \tilde{F} - \ln 5 \right] , \tag{4.10}$$

where ρ_s is the superfluid density in the bulk liquid:

$$\rho_s = 10 \left[\frac{2m_3}{\hbar} \right]^2 K\Delta^2 , \tag{4.11}$$

and R is the external logarithmic cutoff (the radius of the container or the intervortex spacing).

After expressing $\tilde{A}_{\alpha i}$ in terms of $C_{\mu\nu}(r)$,

$$\tilde{A}_{ai} = \sum_{\mu,\nu} a_{\mu\nu} \lambda^\mu_\alpha \lambda^\nu_i , \quad a_{\mu\nu}(\vec{r}) = C_{\mu\nu}(r) e^{i(m-\mu-\nu)\phi} , \tag{4.12}$$

all dependence of the energy density of ϕ disappears due to the axial symmetry and we find

$$\tilde{F} = \int_0^\infty d\tilde{r}\,\tilde{r} \left\{ -C_{\mu\nu} C^*_{\mu\nu} + \tilde{\beta}_1 | C^*_{\mu\nu} C^*_{-\mu-\nu} |^2 + \tilde{\beta}_2 (C_{\mu\nu} C^*_{\mu\nu})^2 + \tilde{\beta}_3 C_{\mu\nu} C^*_{\mu\kappa} C_{\rho-\nu} C^*_{\rho-\kappa} + \tilde{\beta}_4 C^*_{\mu\kappa} C_{\nu\kappa} C^*_{\nu\rho} C_{\mu\rho} + \tilde{\beta}_5 C_{\mu\nu} C_{-\mu\kappa} C^*_{\rho\nu} C^*_{-\rho\kappa} + \sum_{\mu,\nu,\nu'} \left[|\nu| \frac{\partial}{\partial\tilde{r}} C_{\mu\nu} - \nu \frac{(m-\mu-\nu)}{\tilde{r}} C_{\mu\nu} \right] \left[|\nu'| \frac{\partial}{\partial\tilde{r}} C^*_{\mu\nu'} - \nu' \frac{(m-\mu-\nu')}{\tilde{r}} C^*_{\mu\nu'} \right] + \sum_{\mu,\nu} \left[\left| \frac{\partial}{\partial\tilde{r}} C_{\mu\nu} \right|^2 + \left[\frac{m-\mu-\nu}{\tilde{r}} \right]^2 |C_{\mu\nu}|^2 \right] + \frac{3}{2} - \frac{5m^2}{\tilde{r}^2 + r_0^2} \right\} . \tag{4.13}$$

First we consider here the most symmetric o vortex, with one quantum of circulation:

$$a^{(o)}_{\mu\nu}(m=1) = \begin{bmatrix} C_{++} e^{-i\phi} & 0 & C_{+-} e^{i\phi} \\ 0 & C_{00} e^{i\phi} & 0 \\ C_{-+} e^{i\phi} & 0 & C_{--} e^{3i\phi} \end{bmatrix} , \tag{4.14}$$

where all the $C_{\mu\nu}$ are real. At infinity, in the bulk B phase, $C_{++}(\infty) = C_{--}(\infty) = 0$ and $C_{+-}(\infty) = C_{00}(\infty) = C_{-+}(\infty) = 1$. The results of the full minimization are shown in Fig. 3.

Note in Fig. 3 that the most symmetric o vortex has no less than five different nonzero pairing amplitudes. Moreover, even the most symmetric vortex solution is nonunitary. Hence the rotation of superfluid ^{3}He-B which creates vortices also necessarily induces a magnetization of the liquid (see Sec. VII for further details). Observe that in Fig. 3, and in most of the graphs with a radial abscissa in the present paper, the radial scale is linear in r for $r < 5\xi_{GL}$, and it varies as $1/r$ for $r > 5\xi_{GL}$, such that the structure of an isolated vortex line can be represented everywhere: $0 \le r \le \infty$. Because of its normal core structure, the o vortex in Fig. 3 is a weak function of

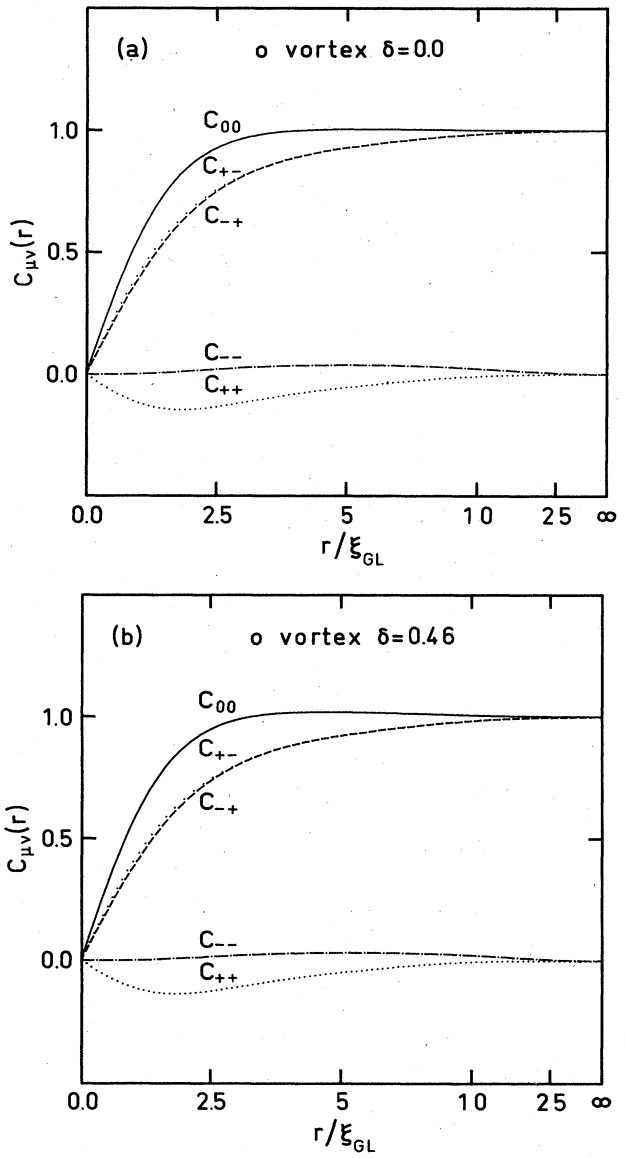

FIG. 3. Structure of the most symmetric singly quantized vortex, the *o* vortex, in superfluid ^{3}He-*B* at (a) the weak-coupling limit with $\delta=0.0$, and (b) the polycritical point where $\delta=0.46$. Here the real pairing amplitudes $C_{\mu\nu}(r)$ (with $C_{\mu\nu}\equiv 0$ for $\mu+\nu$ odd) are scaled such that the bulk ^{3}He-*B* order parameter at $r=\infty$ is described by $C_{+-}(\infty)=C_{00}(\infty)=C_{-+}(\infty)=1$. Radial distances r from the vortex axis are measured in units of the Ginzburg-Landau coherence length $\xi_{GL}(T)=(\frac{3}{5})^{1/2}\xi_0/(1-T/T_c)^{1/2}$. The scale is linear in r for $r<5\xi_{GL}$, and varies as $1/r$ for $r>5\xi_{GL}$, such that the structure of an isolated vortex line can be represented for $0\le r\le\infty$. Note the weak dependence of this normal core vortex on pressure.

pressure; hence the variation with pressure of the normalized *o* vortex susceptibility anisotropy $\tilde{\lambda}$ (see Sec. VI) and the normalized magnetization $\tilde{m}$ (see Sec. VII) is not strong. Computed physical properties associated with the *o* vortex solution are presented in Table II as functions of pressure.

Figure 4 displays the components of the free-energy density in an *o* vortex as functions of the radial distance from the vortex axis. Here (and also in Fig. 8) the asymptote for the total free-energy density in the bulk *B* phase at $r\to\infty$ is $f_{tot}=-1.5$, cf. Eq. (4.8). The (bulk) condensation-energy density, $f_B(r)$, tends to zero on the vortex axis, which is normal. The gradient-energy density $f_G(r)$, obtains its maximum value at $r=0$. This behavior is just as in the classical quantized vortex lines in He II.

The superfluid density $\rho_s(r)$ is a tensor quantity. We consider here the component of ρ_s parallel with the vortex

TABLE II. Calculated properties of the singly quantized *o* vortex (normal core) in superfluid ^{3}He-*B* as functions of the spin-fluctuation parameter δ (cf. Fig. 3). Here the vortex energy is $\pi\rho_s(\hbar/2m_3)^2[\ln(R/\xi_{GL})+E]$ [cf. Eq. (4.10)]. The normalized vortex magnetization equals $\tilde{m}=\int_0^\infty d\tilde{r}\,\tilde{r}\,\tilde{m}(\tilde{r})$, where $\tilde{m}(\tilde{r})=\sum_\nu(C_{+\nu}^2-C_{-\nu}^2)$ [cf. Eq. (7.3)]. The normalized susceptibility anisotropy is given by $\tilde{\lambda}=\int_0^{R/\xi_{GL}} d\tilde{r}\,\tilde{r}\,\tilde{\lambda}(\tilde{r})$, where $\tilde{\lambda}(\tilde{r})=\sum_\nu[C_{0\nu}^2-\frac{1}{2}(C_{+\nu}^2+C_{-\nu}^2)]$ [cf. Eq. (6.11)]. The constant b in this table denotes the integral $b=\int_0^\infty d\tilde{r}\,\tilde{r}[\tilde{\lambda}(\tilde{r})-\tilde{\lambda}_{reg}]$, where the regularizing term is $\tilde{\lambda}_{reg}=(1+3\beta_{12}/\beta_{345})/(\tilde{r}^2+1)$. The constant b may be absorbed as ϵ in the expression for $\tilde{\lambda}$, written as $\tilde{\lambda}=(1+3\beta_{12}/\beta_{345})\ln(R/\epsilon\xi_{GL})$, with $\epsilon=1.067$, 1.079, and 1.114 for $\delta=0.0$, 0.3, and 0.46, respectively. In the table we have chosen the fixed typical value $R=10^4\xi_{GL}$ for the intervortex distance, to ease direct comparison of $\tilde{\lambda}$ with Table III.

δ	E	$\tilde{m}$	$\tilde{\lambda}$	b
0.0	0.023	0.165	22.9	−0.15
0.3	0.021	0.146	26.7	−0.22
0.46	0.018	0.130	29.5	−0.35

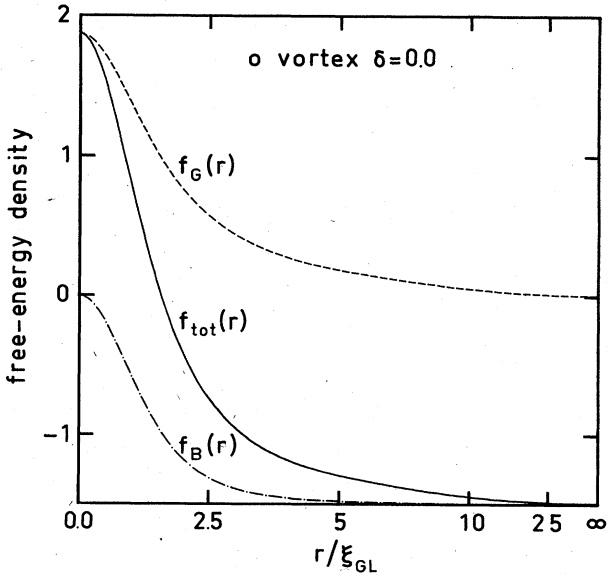

FIG. 4. Radial distribution of the normalized free-energy density for the singly quantized *o* vortex in the weak-coupling limit. Note that because of the normal vortex-core structure, the bulk condensation energy f_B tends to zero for $r\to 0$ and there only remains a finite gradient energy f_G on the vortex axis. The total free-energy density, f_{tot}, is a monotonically decreasing function of r.

axis, $\rho_{s\|}(r)$. The behaviors of the other components are analogous. An expression for $\rho_{s\|}$ is derived easily on calculating the superflow by variation of the vortex free energy with respect to $\vec{v}_s$ (which changes the order parameter $\vec{A}_{\mu\nu} \rightarrow \vec{A}^0_{\mu\nu} e^{i(m_3 \vec{v}_s \cdot \vec{r})/\hbar}$), and finding the linear response of $j_{\|}$ on $v_{s\|}$: $j_{\|}(r) = \rho_{s\|} v_{s\|}$. In the weak-coupling approximation, $K_2 + K_3 = 2K$, $K_1 = K$, we obtain

$$\rho_{s\|}(r) = \rho_s(\infty)\tfrac{1}{5}\left[2\sum_{\mu} |C_{\mu 0}(r)|^2 + \sum_{\mu,\nu} |C_{\mu\nu}|^2\right], \quad (4.15)$$

where $\rho_s(\infty)$ is the (isotropic) bulk superfluid density in the B phase. The superfluid density (4.15), normalized to its bulk value, is displayed in Fig. 5 for the o vortex; the normal core structure is reflected in $\rho_s(r=0)=0$, just as for the classical vortices.

The tangential superflow $j_s(r)$ circulating around the vortex may likewise be derived by variation of the vortex free energy. We find the expression

$$j_s(r) = \tfrac{1}{10}\rho_s(\infty)\frac{\hbar}{2m_3}\tilde{j}_s(r),$$

where the normalized superflow is given for the general axisymmetric singly quantized vortex state in terms of the pairing amplitudes $C_{\mu\nu}$ as follows:

$$\tilde{j}_s(r) = 2\sum_{\nu,\mu}\frac{(1-\nu-\mu)}{r}|C_{\nu\mu}|^2 + \sum_{\mu,\mu',\nu}\left[C^*_{\nu\mu'}C_{\nu\mu}\frac{\mu\mu'}{r}(1-\nu-\mu)+\text{c.c.}\right] + \tfrac{1}{2}\sum_{\mu,\mu',\nu}\left[C^*_{\nu\mu'}\frac{\partial}{\partial r}C_{\nu\mu}(|\mu'|\mu-\mu'|\mu|)+\text{c.c.}\right]. \quad (4.16)$$

The normalized superflow for the o vortex, calculated with the above expression, is illustrated in Fig. 6.

A free-energy minimum, corresponding to a vortex solution in a given symmetry class, is always the extremum of the functional in all of the function space. However, this extremum may not be a true minimum, but rather a saddle point. Therefore, one needs to verify the stability of the solution towards perturbations breaking the o symmetry. We have tested the stability of the o vortex by adding the perturbative parameters $C_{\mu\nu}$ from the u sector, the v sector, and the w sector. We found that while the perturbations from both the u and w sectors decrease to zero in the minimization procedure, the perturbations from the v sector increase, manifesting an instability of the o vortex towards the formation of a v vortex:

$$a^{(v)}_{\mu\nu}(m=1) = \begin{bmatrix} C_{++}e^{-i\phi} & C_{+0} & C_{+-}e^{i\phi} \\ C_{0+} & C_{00}e^{i\phi} & C_{0-}e^{2i\phi} \\ C_{-+}e^{i\phi} & C_{-0}e^{2i\phi} & C_{--}e^{3i\phi} \end{bmatrix}, \quad (4.17)$$

where all the nine functions $C_{\mu\nu}$ ($\mu,\nu = +, 0, -$) are real. The resulting vortex structure, which corresponds to the minimum of the functional (4.13) in the space of the nine real functions $C_{\mu\nu}(r)$, is illustrated in Fig. 7. This vortex state has a superfluid core with A phase (C_{0+} and its dual phase C_{0-}) and a ferromagnetic so-called β phase (C_{+0} and its dual phase C_{-0}) at the vortex axis. This vortex has a lower free energy than the o vortex with normal core (cf. Tables II and III); in fact we have found that at zero magnetic field this superfluid core vortex, which is spontaneously ferromagnetic (and therefore the v vortex magnetization is an order of magnitude larger than for the nonunitary o vortex; see Tables II and III), minimizes the

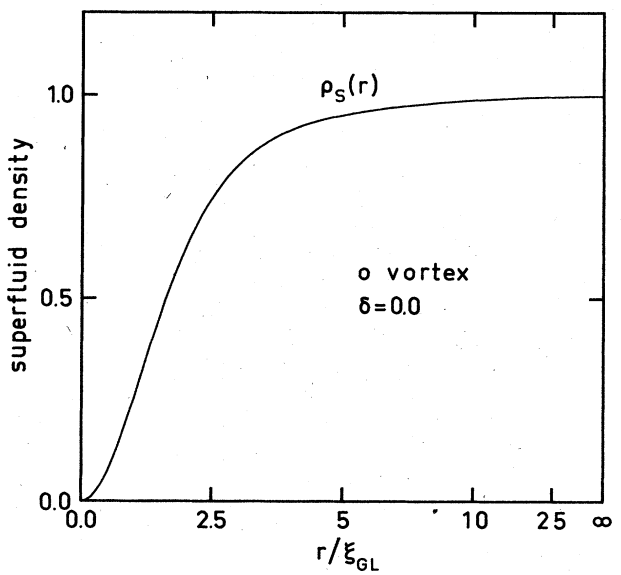

FIG. 5. Calculated normalized superfluid density ρ_s in the o vortex for $\delta=0.0$, presented in Fig. 3(a). This figure shows $\rho_{s\|}$, the component of the superfluid density tensor parallel with the vortex axis. The o vortex core is normal with $\rho_s(r=0)=0$, such as for the classical ^{4}He vortex.

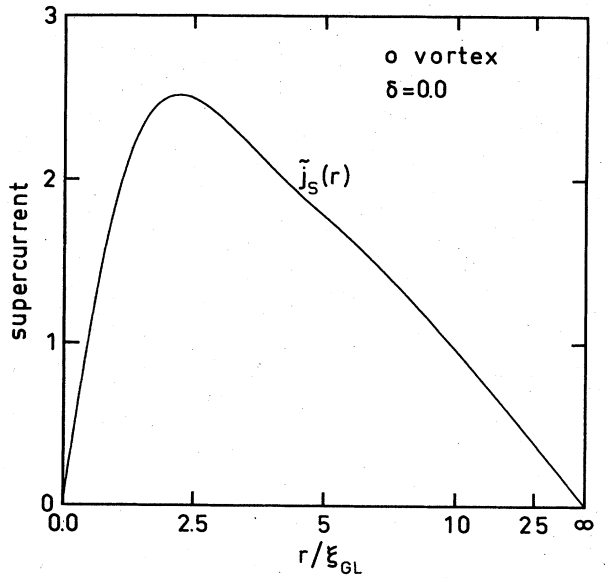

FIG. 6. Computed normalized radial distribution of the tangential supercurrent, $\tilde{j}_s$, for the o vortex in the weak-coupling limit. The linear slope for $r \rightarrow \infty$ results from the asymptotic $1/r$ dependence of the tail of the flow field. The supercurrent decreases for decreasing r close to the vortex axis since ρ_s tends to zero (cf. Fig. 5).

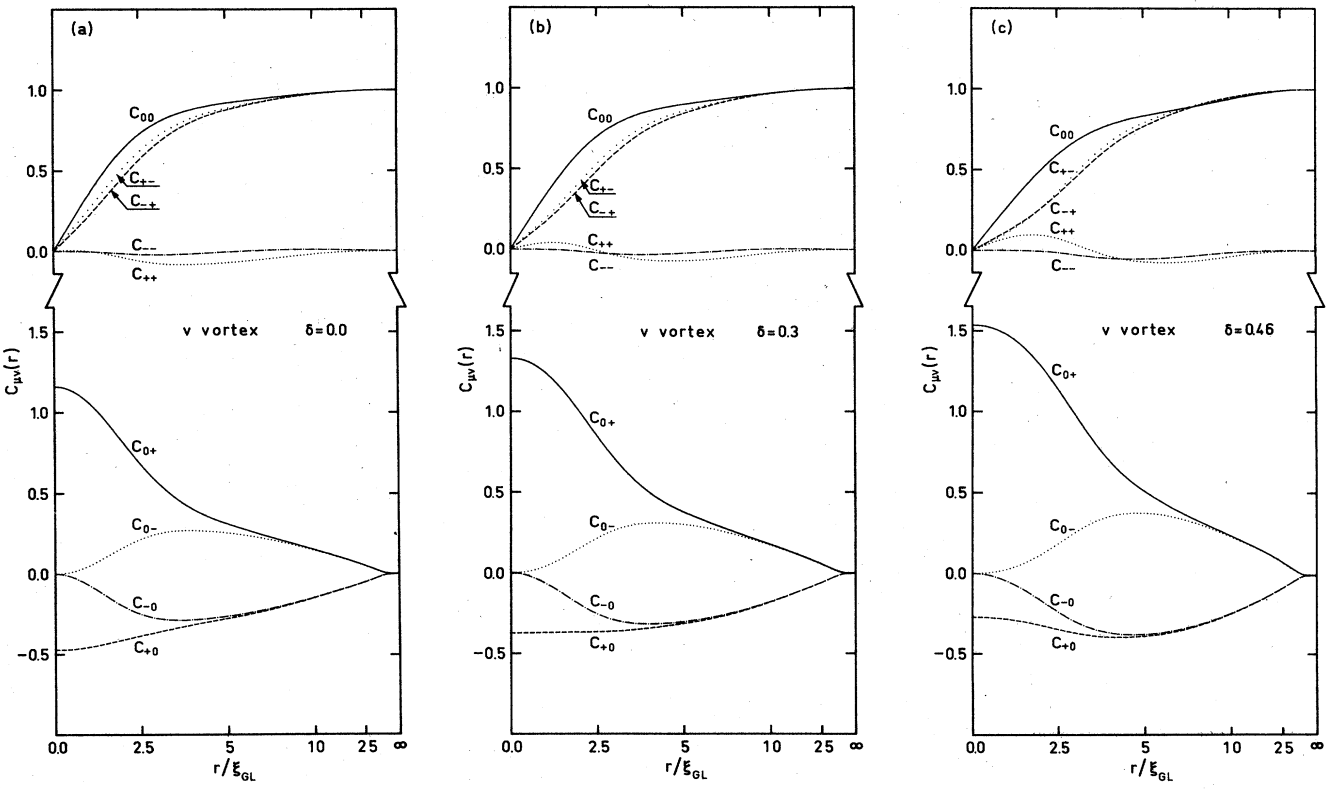

FIG. 7. Calculated structure of the broken-symmetry v vortex as a function of pressure in the Ginzburg-Landau regime. We identify this superfluid core vortex structure as the one observed in the NMR experiments on rotating bulk superfluid ^{3}He-B in low magnetic field for $T\rightarrow T_c$ at all pressures. The upper curves represent the same five different pairing amplitudes $C_{\mu\nu}(r)$ (for $\mu+\nu$ even) that also occur in the maximally symmetric o vortex; the lower curves display the four additional pairing amplitudes $C_{\mu\nu}(r)$ (with $\mu+\nu$ odd) (A phase and the ferromagnetic β phase and their dual phases) that exist in this P_2 symmetric vortex structure. The scales are as in Fig. 3. (a) Weak-coupling (zero pressure) limit, $\delta=0.0$. (b) Intermediate pressures, $\delta=0.3$. (c) Polycritical point, $\delta=0.46$. Note that, contrary to the o vortex displayed in Figs. 3, the structure of this v vortex is a strong function of δ; in particular, the superfluid core depends sensitively on pressure. Further derived data on the v vortex is presented in Figs. 8–16, and in Table III. Observe that far from the core $C_{0+}\approx C_{0-}$ and $C_{-0}\approx C_{+0}$; $C_{+-}\approx C_{-+}$ and $C_{++}\approx C_{--}$, due to an approximate time inversion (T) symmetry: $t\rightarrow -t$.

free-energy functional in Eq. (4.13) for the class of singly quantized axisymmetric vortices for all values of the coefficients (β_1 to β_5) of the fourth-order invariants corresponding to stable bulk B phase. [Observe that for $\delta=0$ the normalized A-phase pairing amplitude C_{0+} has the value $C_{0+}(r=0)=1.17$ on the vortex axis, rather than the less accurate value 1.02 obtained in the solution quoted in the first report, Ref. 8. However, this slight numerical inaccuracy is both qualitatively and quantitatively unimportant.]

TABLE III. Computed physical properties of an isolated v vortex (ferromagnetic superfluid core) in superfluid ^{3}He-B as functions of δ (cf. Fig. 7). The vortex energy E and the normalized magnetization $\tilde{m}$ are as defined in the caption to Table II. The v-vortex core radius $r_{\rm core}$ is determined as the distance where boojums (nodes) in the ^{3}He quasiparticle energy gap first appear on the Fermi sphere (cf. Figs. 12–14), and the superflow becomes nonpotential. Here $\tilde{\lambda}_{\rm tot}=\int_0^{R/\xi_{GL}} d\tilde{r}\,\tilde{r}\,\tilde{\lambda}(\tilde{r})$ is divided up into two different contributions: the flow term $\tilde{\lambda}_{\rm flow}$ and the term due to the vortex core anisotropy, $\tilde{\lambda}_{\rm core}$. The flow term is $\tilde{\lambda}_{\rm flow}=(1+3\beta_{12}/\beta_{345})\ln(R/r_{\rm core})$, while the core anisotropy term is $\tilde{\lambda}_{\rm core}=\tilde{\lambda}_{\rm tot}-\tilde{\lambda}_{\rm flow}$. The numbers for $\tilde{\lambda}$ were again calculated using $R=10^4\xi_{GL}$.

δ	E	$\tilde{m}$	$r_{\rm core}/\xi_{GL}$	$\tilde{\lambda}_{\rm tot}$	$\tilde{\lambda}_{\rm flow}$	$\tilde{\lambda}_{\rm core}$
0.0	−0.014	1.59	1.9	25.3	21.4	3.9
0.1	−0.0145	1.58	2.1	27.3	22.2	5.1
0.2	−0.015	1.56	2.2	29.1	23.2	5.9
0.3	−0.020	1.44	2.35	31.8	24.4	7.4
0.4	−0.030	1.35	2.55	34.9	25.7	9.2
0.46	−0.036	1.47	3.1	39.6	26.1	13.5

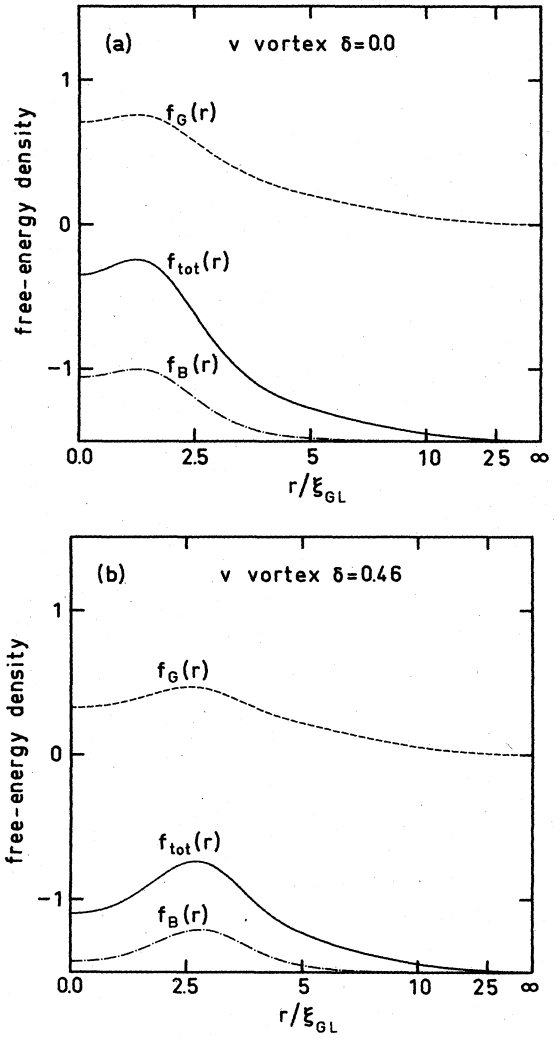

FIG. 8. Components of free-energy density in the superfluid core v vortex. Note that the bulk condensation energy f_B remains finite everywhere. (a) For $\delta=0.0$ the condensation-energy density is diminished by 29% from its bulk equilibrium value, while (b) for $\delta=0.46$ the condensation-energy loss on the vortex axis from its bulk value is only 6%, since for this value of δ the transition to the A phase in bulk superfluid ^{3}He is in close proximity. The gradient energy f_G is greatly diminished at $r=0$ from that of the o vortex in Fig. 4 because of the escape of the superfluid into other pairing states. Note that the total energy density f_{tot}, as well as the bulk condensation-energy density f_B, exhibit extremal values at a finite distance from the vortex axis. This may be visualized as resulting from a domain wall which separates the bulk B phase from the A phase in the vortex core.

Figure 7 shows the change in the structure of the v vortex with increasing strong-coupling parameter δ. A most interesting behavior is that of the superfluid core at $\delta=0.46$, in the immediate vicinity of the polycritical point, where the B phase is about to become metastable in the bulk liquid and the A phase becomes stable. With further increase of δ, the amplitude of C_{0+} of the A phase component in the core begins to increase towards its bulk-liquid value in the A phase:

$$C_{0+}^{\text{bulk}}=\left[\frac{3\beta_{12}+\beta_{345}}{\beta_{345}}\right]^{1/2}=\left[\frac{5-\delta}{2-1.05\delta}\right]^{1/2}, \tag{4.18}$$

while the β phase amplitude decreases for increasing values of δ right on the vortex axis (however, the extension of the β phase increases dramatically in the outer core region, resulting in roughly the same integrated value for the normalized vortex magnetization; see Sec. VII and Table III). That is, the vortex core becomes bulk A phase. The extension of this A-phase nucleation center increases with δ. This means that the vortex in the B phase is the center of nucleation of the stable A phase in the metastable B phase. Because of the large amplitudes of the A and β phases in the v vortex, the five pairing amplitudes C_{++}, C_{+-}, C_{00}, C_{-+}, and C_{--}, which already exist in the o vortex, are strongly and nonlinearly modified by the presence of the amplitudes C_{+0}, C_{0+}, C_{0-}, and C_{-0} and cannot simply be considered to provide a potential for the four additional components.

The free-energy density in the v vortex is shown in Fig. 8. The bulk condensation energy $f_B(r)$ remains finite everywhere, and the gradient energy $f_G(r)$ is appreciably reduced on the vortex axis from its value in the o vortex (Fig. 4) because of the escape of the superfluid into the other pairing states. The total energy f_{tot} displays an extremal value at a finite distance from the vortex axis. This can be interpreted to result from a domain wall separating the bulk B phase from the A phase nucleated at the vortex core. For $\delta=0.0$ [Fig. 8(a)], the domain wall is close to the vortex axis, and the A phase in the core results in appreciably higher condensation energy than in the bulk B phase. At $\delta=0.46$ [Fig. 8(b)], however, the A phase in the core results in almost the same low

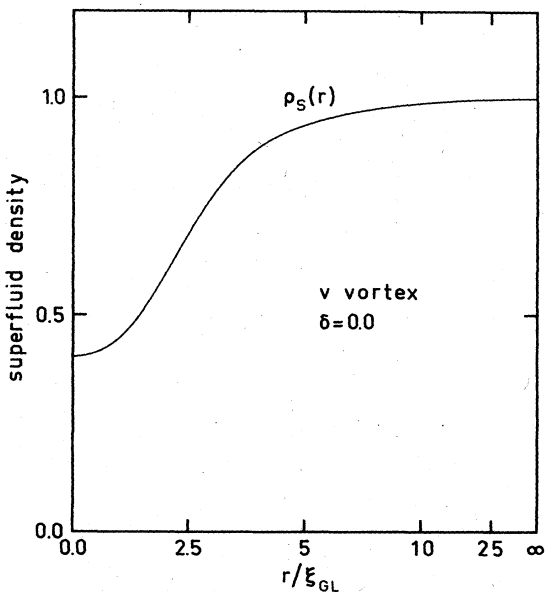

FIG. 9. Component of the normalized superfluid density along the vortex axis, calculated for the v vortex in Fig. 7(a). Note that unlike for the o vortex (Fig. 5), here the superfluid density remains finite everywhere, including the vortex axis. This is because of the superfluid core structure of this quantized vortex line.

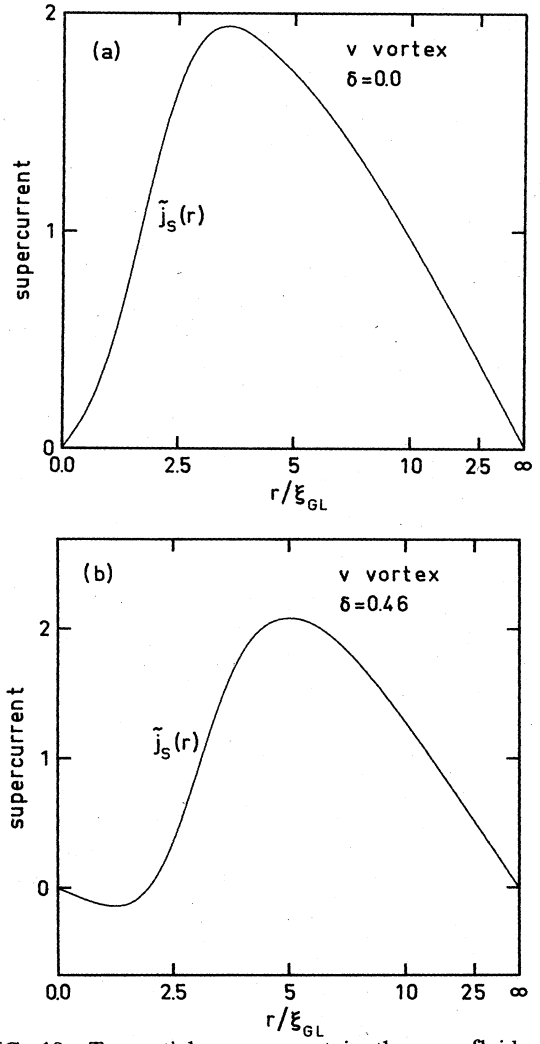

FIG. 10. Tangential supercurrent in the superfluid core v vortex. (a) Weak-coupling limit, $\delta=0$ [cf. Fig. 7(a)]. (b) Strong-coupling limit, $\delta=0.46$ [cf. Fig. 7(c)]. Here the superflow tends to the potential-flow regime only for radial distances $r>r_{\rm core}$ from the vortex axis, where the vortex core radii are given in Table III. For $r<r_{\rm core}$, the superflow distribution is governed by the nodes of the energy gap on the Fermi sphere. In particular, note how in case (b), close to the vortex axis, there is a region where the superflow is counterrotating. Since $\rho_s(r=0)$ remains finite (Fig. 9), while $\tilde{j}_s$ tends to zero at $r\to 0$, this may be visualized as a solid-body rotation of the superfluid near the vortex axis.

condensation-energy minimum as in the B phase. The vortex core radius is much increased and the domain wall separating the superfluids in the bulk and in the vortex-core region is more pronounced.

The normalized superfluid density for the v vortex is shown in Fig. 9. Unlike the o vortex or the classical vortex in He II, this v vortex possesses a finite superfluid density everywhere, including the vortex axis, in particular.

Figure 10 illustrates the distribution of the supercurrent in the v vortex. In the vortex core, the nucleation of the superfluid A phase leads to the appearance of nodes in the ^{3}He quasiparticle energy gap (local $\vec{l}$ vector field with its associated superfluid flow properties). This results in vortices in $\hat{p}$ space, which are discussed in the following section.

Due to its symmetries, P_2 and Q, the v vortex solution described above is also an extremum of the total vortex energy functional. However, its instability to further breaking of symmetry has not yet been excluded. We only want to note in this connection that an axial asymmetry combined with the already broken parity P of the v vortex will produce a twist. Let $\hat{\nu}$ be the direction of the vortex anisotropy in the x-y plane, then the absence of the symmetry P allows for the existence of a free-energy term proportional to $\vec{\nu}\cdot\vec{\nabla}\times\vec{\nu}$, as in cholesteric liquid crystals. This will result in a twisted vortex texture with broken translational symmetry t_z:

$$\hat{\nu}=\hat{x}\cos(qz)+\hat{y}\sin(qz)\ . \tag{4.19}$$

In the future, we shall investigate in detail perturbations breaking the symmetry P_2, and nonaxial perturbations.

V. TOPOLOGY OF THE ENERGY GAP IN THE VORTEX CORE

The structure of the vortex core in the B phase is intimately related with the properties of the ^{3}He quasiparticle spectrum inside the core, and in particular with the topology of the nodes in the energy gap.[27] In triplet pairing there are in general two branches of the quasiparticle excitation spectrum:

$$E_\uparrow=[\,|\,\Delta_\uparrow(\hat{p})\,|^2+v_F^2(p-p_F)^2]^{1/2}\ , \tag{5.1a}$$

$$E_\downarrow=[\,|\,\Delta_\downarrow(\hat{p})\,|^2+v_F^2(p-p_F)^2]^{1/2}\ , \tag{5.1b}$$

which correspond to the two possible opposite spin projections of the ^{3}He quasiparticle. Here $\hat{p}$ is the unit vector along the ^{3}He quasiparticle momentum $\vec{p}$. The direction of the quasiparticle spin quantization axis and the magnitudes of the gaps $\Delta_\uparrow(\hat{p})$ and $\Delta_\downarrow(\hat{p})$ are obtained after the diagonalization of the 2×2 gap matrix $\hat{\Delta}(\hat{p})$:

$$\hat{\Delta}(\hat{p})=i\hat{\sigma}_2\hat{\sigma}_\alpha A_{\alpha i}\hat{p}_i\ , \tag{5.2}$$

$$\hat{U}\hat{\Delta}(\hat{p})\hat{U}^\dagger=\begin{bmatrix}\Delta_\uparrow(\hat{p}) & 0\\ 0 & \Delta_\downarrow(\hat{p})\end{bmatrix}\ , \tag{5.3}$$

where $\hat{U}(\hat{p},\vec{r})$ is a unitary transformation.

The nodes of the energy gaps for an arbitrary order parameter $A_{\alpha i}$ may be found from a consideration of the determinant of the gap matrix $\hat{\Delta}(\hat{p})$:

$$\det[\hat{\Delta}(\hat{p})]=-A_{\alpha i}\hat{p}_i A_{\alpha j}\hat{p}_j=\Delta_\uparrow(\hat{p})\Delta_\downarrow(\hat{p})\ . \tag{5.4}$$

If for a given $\hat{p}$ we find that $\det[\hat{\Delta}(\hat{p})]=0$, then for this $\hat{p}$ at least one of the gaps $\Delta_\uparrow$ or $\Delta_\downarrow$ is zero.

For the bulk B phase, with its order parameter given in Eq. (3.3), one finds

$$\det(\hat{\Delta})=-\Delta^2(T)\ , \tag{5.5}$$

and there are no nodes in the energy gap.

For the bulk A phase, with the order parameter [here $\Delta_A(T)$ denotes the amplitude of the energy gap]

$$A_{\alpha i}=\Delta_A(T)d_\alpha(\Delta_i'+i\Delta_i''), \tag{5.6}$$

both species of ^{3}He quasiparticles, with respective spin projections $\pm\frac{1}{2}$ on the spin quantization axis $\vec{d}$, have a node at $\hat{p}$ parallel with the orbital quantization axis $\vec{l}=\vec{\Delta}'\times\vec{\Delta}''$. The corresponding determinant is

$$\det[\hat{\Delta}(\hat{p})]=\Delta_A^2(T)[(\vec{\Delta}''\cdot\hat{p})^2-(\vec{\Delta}'\cdot\hat{p})^2 -2i(\vec{\Delta}'\cdot\hat{p})(\vec{\Delta}''\cdot\hat{p})], \tag{5.7}$$

$$|\det[\hat{\Delta}(\hat{p})]|=\Delta_A^2(T)(\hat{p}\times\hat{l})^2 .$$

The nodes in the energy gap define all the superfluid properties of ^{3}He, including the peculiar continuous vorticity of superflow. The important point to emphasize here is that these nodes of the gap are just such points on the Fermi surface around which the phase of $\det[\hat{\Delta}(\hat{p})]$ changes by $2\pi N$, where N denotes an integer ($N=2$ for $\det[\hat{\Delta}(\hat{p})]$ in the A phase given by Eq. (5.7)). Such point vortices on the Fermi surface are called boojums,[27] because they resemble those point singularities in real space, which may occur on the surface of a container, that were first introduced by Mermin.[28] These vortices in the $\hat{p}$ space and the more common vortices in the $\vec{r}$ space have basically the same origin: They are vortices in the order-parameter field $\hat{\Delta}(\hat{p},\vec{r})$, and therefore they may transform to each other by the deformation of the order parameter both in the $\hat{p}$ and in the $\vec{r}$ spaces. Due to these transformations, singular vorticity of the quantized vortex in $\vec{r}$ space may be smoothened by "flaring out" of the vortex in $\hat{p}$ space. We illustrate this in the present paper on the example of the singly quantized v vortex; the doubly quantized axisymmetric vortices also display similar properties, see Refs. 15 and 16.

Note that the singly quantized o vortex has no nodes in the gap anywhere across the core, for $\det[\hat{\Delta}(\hat{p})]$ never goes to zero. Hence there are no boojums on the Fermi surface and vorticity in the singly quantized o vortex is strictly singular: the circulation of superflow along any path embracing the vortex axis is 2π, irrespective of the path chosen, and the superfluid velocity has a singularity on the vortex axis, where the gap vanishes: $\hat{\Delta}(\hat{p},\vec{r}=0)=0$ all over the Fermi surface, giving rise to the normal state at the vortex axis.

The situation is fundamentally different for the v vortex, where this singularity is resolved through the formation of vortices in $\hat{p}$ space, with the result that superfluidity is not broken on the vortex axis. However, topological analysis predicts that in order to escape the singularity on the vortex axis, two pairs of boojums associated with the opposite topological charges $N=\pm1$ should appear at the Fermi surface for some finite distance from the vortex axis. Here we choose to denote this distance where the nodes in the ^{3}He quasiparticle excitation spectrum first appear as the vortex core radius ($r_{\rm core}$), since everywhere in the core region inside this radius the superflow is nonpotential.

For decreasing distances $r<r_{\rm core}$ from the vortex axis, these boojums must move continuously to the poles of the Fermi surface, while covering on their way all the Fermi surface. Finally, on reaching the vortex axis, the nodes fuse together at $r=0$ on the poles, where they produce antipodal boojums with the net topological charges $N=\pm2$, which correspond to the superfluid A phase on the vortex axis.

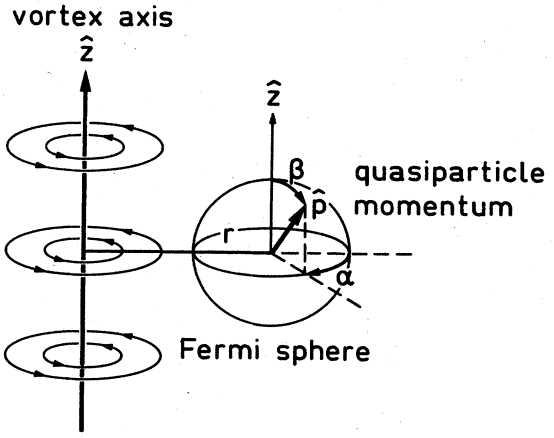

FIG. 11. Illustration of the local angles $\alpha(r)$ and $\beta(r)$ that are used in Eq. (5.8) to define the directions of quasiparticle momentum $\hat{p}$ on the Fermi sphere, where one of the two energy gaps disappears.

The maximum number of boojums on the Fermi sphere is not four for p-wave pairing, as was stated erroneously

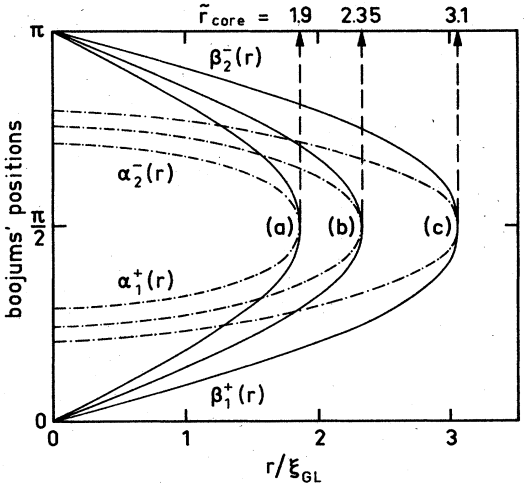

FIG. 12. Angles $\alpha(r)$ and $\beta(r)$, obtained as solutions of Eqs. (5.10), which determine the positions of boojums (nodes) in the ^{3}He quasiparticle energy gap on the Fermi sphere for the singly quantized v vortex. The three sets of curves (a,b,c) correspond to the three different v vortex structures shown in (a), (b), and (c) of Fig. 7. (a) $\delta=0.0$. (b) $\delta=0.3$. (c) $\delta=0.46$. Also indicated in this figure is the vortex core radius, $r_{\rm core}$, which in this paper is defined as that distance at which nodes in the ^{3}He quasiparticle energy gap first appear. The core radius is measured in units of the Ginzburg-Landau coherence length: $\tilde{r}=r/\xi_{\rm GL}$. The angles α_1^+ and β_1^+ refer to the position of boojum 1^+ with unit positive topological charge, while α_2^- and β_2^- refer to the boojum 2^- with unit negative topological charge. At $r=r_{\rm core}$ these two boojums with opposite charges annihilate each other.

in Ref. 27, but rather twice as many. The latter result of eight possible nodes of the gap follows on taking into account the complex nature of the object $\det[\hat{\Delta}(\hat{p})]$. Therefore, another two pairs of nodes may appear (and disappear) on the Fermi sphere. However, they must cover zero net area on the Fermi surface (provided that one takes into account the sign of the surface orientation). This follows because of the topological requirement that for a continuous distribution of the order parameter inside the core of the singly quantized vortices, the total area of the Fermi surface covered by all the boojums with positive charges $N=+1$ should equal $4\pi p_F^2$ (or, more generally, $4\pi m p_F^2$ for the case of an m times quantized continuous vortex).

Let us now illustrate these topological concepts here on the example of the singly quantized v vortex structure obtained in Sec. IV. Specifically, let us find how the positions of the boojums on the Fermi surface in the v vortex depend on the coordinate $\vec{r}=(r,\phi)$ in (real) space. Since the v vortex is axially symmetric, the positions of the boojums are determined by the two parameters $\alpha(r)$ and $\beta(r)$:

$$\hat{p}(\vec{r})=\hat{z}\cos[\beta(r)]+\sin[\beta(r)]\{\hat{r}\cos[\alpha(r)]+\hat{\phi}\sin[\alpha(r)]\}\ . \tag{5.8}$$

Here β and α denote the polar and the azimuthal angles on the Fermi sphere, where $\beta(r)$ is measured with respect to the axis ($\hat{z}$) of the vortex, while $\alpha(r)$ is measured with respect to the direction $\hat{r}$ of the radius vector in real space (for an illustration, see Fig. 11).

These parameters $\alpha(r)$ and $\beta(r)$ obey the following equation at directions where the gap nodes occur:

$$\det[\hat{\Delta}(\hat{p})]=0\ . \tag{5.9}$$

As noted above, this equation may in the general case possess eight different solutions. The first four possible vortices are obtained as solutions of the following pair of coupled equations:

$$\tan^2\beta=\frac{2}{e}\left[f-\frac{a}{b}\left[c-\frac{a}{b}d\right]\right]\ , \tag{5.10a}$$

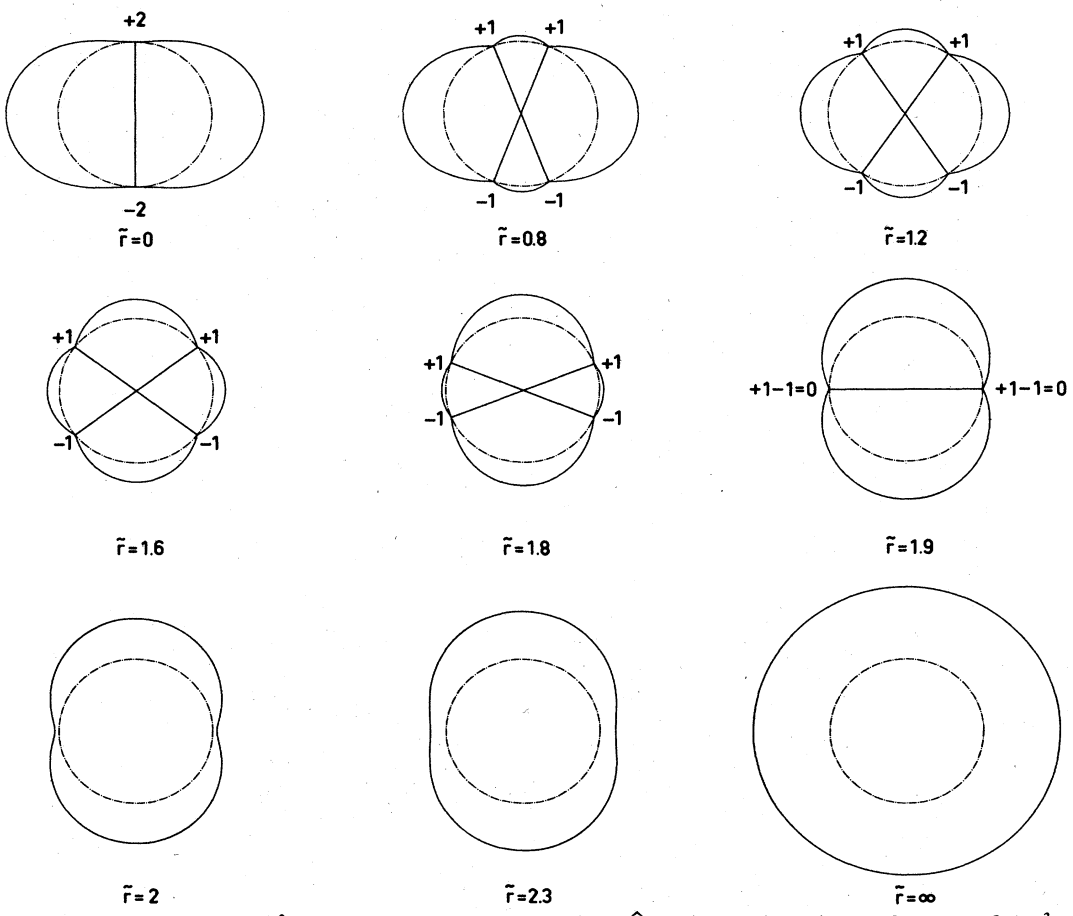

FIG. 13. Computed magnitude of the ^{3}He quasiparticle energy gap $|\det[\hat{\Delta}(\hat{p})]|=\Delta_\uparrow(\hat{p})\Delta_\downarrow(\hat{p})$ as a function of the ^{3}He quasiparticle momentum and the radial distance $r=\tilde{r}\xi_{GL}$ from the vortex axis. For $r<r_{core}$ we choose the cross-sectional plane of the Fermi surface such that it contains all the four different nodes; this plane can be readily visualized with the aid of Figs. 11 and 12. For $r=0$ there is a pair of boojums on the antipodal points with double topological charges, $N=\pm 2$. For $r>0$ these divide up into two pairs of boojums, each carrying unit topological charges, $N=\pm 1$. For increasing r the boojums move continuously towards the equatorial plane, where they annihilate each other ($+1-1=0$) at $r=r_{core}$, displayed in Fig. 12. For $r>r_{core}$, the energy gap is strongly anisotropic, but no more nodes exist. For $r\to\infty$ one obtains the isotropic B-phase energy gap.

$$\cos\alpha = -\sqrt{2}\left[\frac{a}{b}\right]\cot\beta\ , \tag{5.10b}$$

where

$$a = \sum_{\mu,\nu} \nu C_{-\mu 0} C_{\mu\nu}\ , \tag{5.11a}$$

$$b = \sum_{\mu,\nu} \nu C_{\mu\nu} C_{-\mu\nu}\ , \tag{5.11b}$$

$$c = \sum_{\mu,\nu} |\nu| C_{-\mu 0} C_{\mu\nu}\ , \tag{5.11c}$$

$$d = \sum_{\mu,\nu} |\nu| C_{\mu\nu} C_{-\mu\nu}\ , \tag{5.11d}$$

and

$$e = \tfrac{1}{2}\left[d - \sum_{\mu,\nu}(|\nu| C_{\mu\nu} C_{-\mu-\nu})\right]\ . \tag{5.11e}$$

Another set of four possible solutions is determined by the equations

$$\sin\alpha = 0\ , \tag{5.12a}$$

$$\tan\beta = 2\sqrt{2}\left[\frac{-c \pm (c^2 - gf)^{1/2}}{g}\right]\ , \tag{5.12b}$$

where

$$f = \sum_{\mu} C_{\mu 0} C_{-\mu 0}\ , \tag{5.11f}$$

and

$$g = \tfrac{1}{2}\left[d + \sum_{\mu,\nu}(|\nu| C_{\mu\nu} C_{-\mu-\nu})\right]\ . \tag{5.11g}$$

On inserting the parameters $C_{\mu\nu}(r)$ for the v vortex obtained in Sec. IV to the above equations (5.12), we find that there is no radius r at which there would exist a solution of these equations.

However, there are solutions of Eqs. (5.10) for $r \le r_{\rm core}$, where the core radius is given in Table III for different values of δ. These solutions represent two pairs of boojums on the Fermi sphere. One pair contains the boojum 1^+ with the topological charge $N=+1$ and with the angles $\beta_1^+(r)$ and $\alpha_1^+(r)$ (illustrated in Fig. 12 for three different values of the spin-fluctuation parameter), and the diametrically opposite boojum 1^- with the topological charge $N=-1$ and with the corresponding angles $\beta_1^-(r)=\pi-\beta_1^+(r)$ and $\alpha_1^-(r)=\pi+\alpha_1^+(r)$. The respective positions of the second pair of boojums, 2^- and 2^+, are given by

$$\beta_2^-(r)=\pi-\beta_1^+(r)\ ,\quad \alpha_2^-(r)=\pi-\alpha_1^+(r) \tag{5.13}$$

and

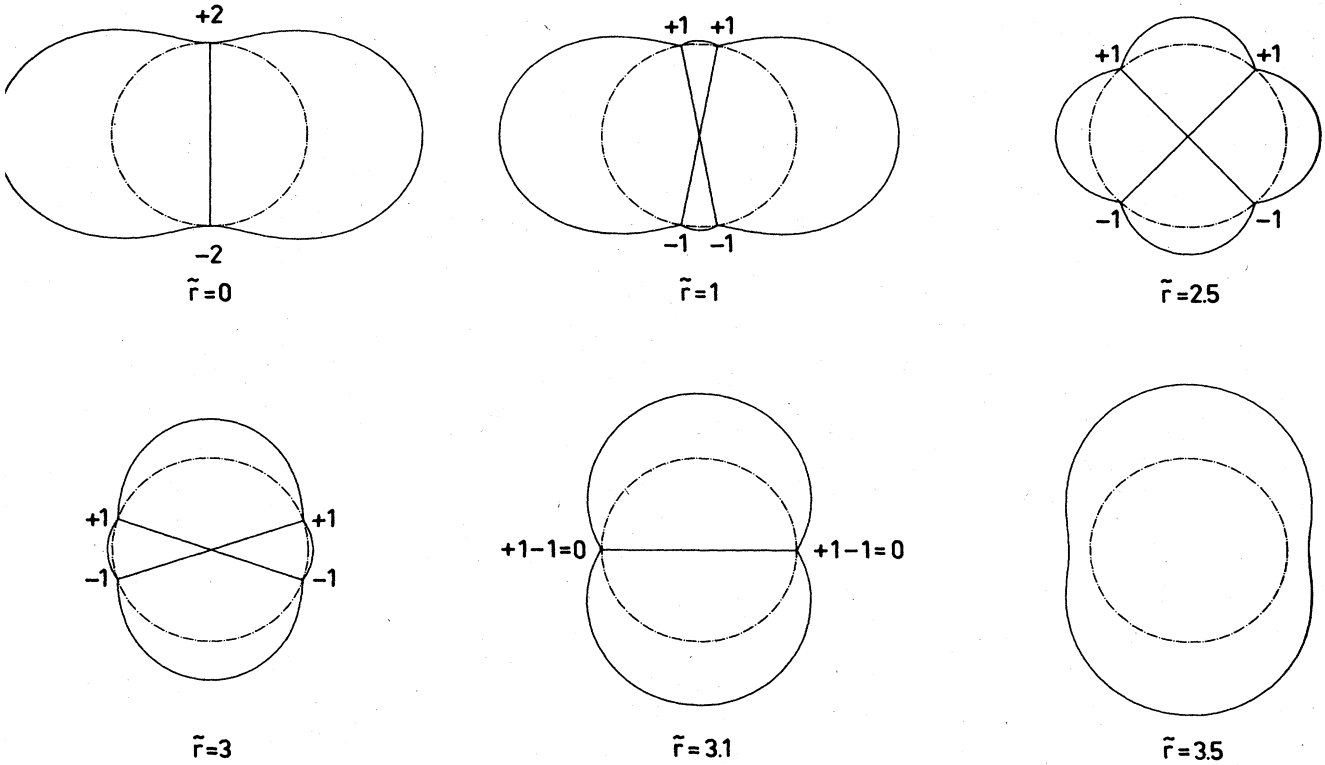

FIG. 14. Calculated gap $|\det[\hat{\Delta}(\hat{p})]|$ for the v vortex with $\delta=0.46$, at the polycritical pressure, illustrated in Fig. 7(c). Note that in the present case the vortex core radius is much increased, and in particular that on the vortex axis the magnitude of the ^{3}He quasiparticle energy gap is significantly in excess of its value in the bulk superfluid B phase. This leads to reflection of ^{3}He quasiparticles off the v vortex core, and thus influences the mutual friction coefficient in rotating superfluid ^{3}He-B.

$$\beta_2^+(r)=\beta_1^+(r)\ ,\quad \alpha_2^+(r)=-\alpha_1^+(r)\ . \tag{5.14}$$

The angles $\beta_2^-(r)$ and $\alpha_2^-(r)$ of the boojum 2^- are also shown in Fig. 12. At the vortex core radius the boojums 1^+ and 2^- mutually annihilate each other, and also the boojums 2^+ and 1^- coalesce together, such that no boojums remain for distances $r>r_{\rm core}$ from the vortex axis.

Figure 13 illustrates computed cross sections of the Fermi surface for the v vortex in the weak-coupling limit shown in Fig. 7(a). Here $|\det[\hat{\Delta}(\hat{p})]|$ is drawn in the plane which contains all the four nodes. These cross sections are given for several different chosen distances r from the vortex axis. Note that for $r>r_{\rm core}$, the magnitude $|\det(\hat{\Delta})|$ is represented in the equatorial plane ($\beta=\pi/2$), where the nodes first appear at $r=r_{\rm core}$. This figure displays the process of splitting of the boojums on the antipodal points with the topological charges $N=\pm 2$ at $r=0$ into two pairs of boojums, each with $N=\pm 1$, at $r>0$. For r tending to $r_{\rm core}$, the boojums move towards the equator, where the opposite topological charges annihilate each other at $r=r_{\rm core}$. Indeed, we verify that the boojums with a positive topological charge do cover the Fermi surface once, on taking into account the orientation of the covering surface.

Figure 14 is a similar display of the boojums on the Fermi sphere for the v vortex at the polycritical point with $\delta=0.46$, displayed in Fig. 7(c). Note the increased core radius with increasing δ. Moreover, we here find the interesting feature that the amplitude of the ^{3}He quasiparticle energy gap is clearly larger on the vortex axis at the equatorial directions on the Fermi sphere than the value of the gap in the bulk B phase at $r=\infty$.

The features described above serve to render the problem of the scattering of superfluid ^{3}He quasiparticle excitations off the quantized vortex line in superfluid ^{3}He-B an interesting one. Solution for the ^{3}He quasiparticle scattering states enters the calculation of the coefficient of the mutual friction of the vortex lines with the liquid ^{3}He.[29] Unlike in vortices of ordinary s-wave superconductors, the solutions of the Bogoliubov–de Gennes equations here yield a spectrum of bound fermion quasiparticle states[29] for finite distances $r\le r_{\rm core}$, not only on the vortex axis.

VI. EFFECT OF THE VORTEX CORE ON THE NMR SIGNAL

The basic interaction determining the NMR properties of the superfluid B phase is the weak spin-orbit (dipolar) force:

$$F_D=g_D(A_{ii}^*A_{jj}+A_{ij}^*A_{ji}-\tfrac{2}{3}A_{ij}^*A_{ij})\ , \tag{6.1}$$

with

$$g_D=\frac{\pi}{10}\left[N(0)\gamma\hbar\ln\left[\frac{E_F}{T_c}\right]\right]^2$$

in the weak-coupling limit. This interaction partially lifts the degeneracy of the bulk ^{3}He-B order parameter in Eq. (3.3). Only those matrices $R_{ai}(\vec{n},\theta_0)$ which describe the rotation of the spin and orbital axes relative to each other about an arbitrary axis $\vec{n}$ but by the fixed, so-called "magic angle" $\theta_0=\arccos(-\frac{1}{4})$, correspond to the minimum of the dipole energy:

$$R_{ai}(\vec{n},\theta_0)=\tfrac{1}{4}(-\delta_{ai}+5n_an_i-\sqrt{15}e_{aik}n_k)\ . \tag{6.2}$$

The dipole interaction gives rise to the transverse NMR shift from the Larmor precession frequency $\omega_0=|\gamma|H$ (here γ denotes the gyromagnetic ratio for ^{3}He), which depends on the mutual orientations of $\vec{n}$ and the magnetic field $\vec{H}$. At the high magnetic field employed in the experiments, $H\gg 25$ G, the NMR frequency shift is given by

$$\omega-\omega_0=\frac{\Omega_B^2}{2\omega_0}(\vec{n}\times\hat{H})^2\ ,\quad \hat{H}=\frac{\vec{H}}{H}\ , \tag{6.3}$$

where Ω_B is the Leggett frequency (see, for example, Ref. 30). Therefore, the frequency shift reflects the $\vec{n}$ texture resulting from the combined action of the dipole force, the magnetic field, and the vortices.[31–34] This makes it possible to investigate the properties of the vortices by extracting the vortex contribution to the NMR signal, which is proportional to the number density of the vortices, and therefore to the angular velocity of rotation of the sample.[1–3]

However, prior to considering in detail the influence of the vortices on the $\vec{n}$ vector texture, let us first find out whether the dipole energy and the magnetic field influence the structure of an isolated vortex. The magnetic energy is

$$F_H=\frac{1}{2}\frac{(\chi_N-\chi_B)}{\Delta^2}A_{ai}A_{\beta i}^*H_\alpha H_\beta\ , \tag{6.4}$$

where χ_N and χ_B are the magnetic susceptibilities of the normal phase and the bulk B phase, respectively. The dipole energy and the magnetic field term produce the following combined effect on the $\vec{n}$ texture:

$$F_{DH}=-a(\vec{n}\cdot\vec{H})^2\ ,\quad a=\frac{5}{8}\frac{g_D(\chi_N-\chi_B)}{\Delta^2\beta_{345}}\ . \tag{6.5}$$

Each of the above interactions, F_D, F_H, and F_{DH}, is characterized by its healing length:

$$\xi_D=\left[\frac{K}{g_D}\right]^{1/2}\sim 10^{-3}\ {\rm cm}\ , \tag{6.6a}$$

$$\xi_H=\left[\frac{2K\Delta^2}{(\chi_N-\chi_B)H^2}\right]^{1/2}\sim\xi_D\frac{25\ {\rm G}}{H}\ , \tag{6.6b}$$

$$\xi_{DH}=\frac{\xi_D\xi_H}{\xi_{\rm GL}}\ . \tag{6.6c}$$

At distances $r>\xi_{DH}$ from the vortex axis, the asymptotic form of the order parameter is given by Eq. (3.7), with $\theta=\theta_0$ and $\vec{n}\|\vec{H}$, in order to minimize F_D and F_{DH}. Is this asymptotic behavior different at distances less than ξ_{DH}, but larger than $\xi_{\rm GL}$? The comparison of the gradient energy with the energies F_H, F_D, and F_{DH} shows (see also Refs. 35) that at sufficiently low fields, obeying

$$\xi_H^2 > \xi_{GL}^2 \ln\left[\frac{\xi_{DH}}{\xi_{GL}}\right], \tag{6.7}$$

the asymptotics is the same everywhere. That is, the vortex structure even far from the central core region possesses rigidity. The rigidity disappears at larger fields, where the vortex structure becomes more complicated. At these higher field strengths, with

$$\xi_H^2 \lesssim \xi_{GL}^2 \ln\left[\frac{\xi_{DH}}{\xi_{GL}}\right],$$

the ^{3}He-B vortex possesses two cores as in the A phase: a hard core of the size of several ξ_{GL} and a soft core of the extent ξ_D. In the soft core, the $\vec{n}$ vector is oriented by the combined actions of the superflow around the vortex and the magnetic field; outside this soft core $\vec{n}$ is oriented along $\vec{H}$ by the combined action of the magnetic field and dipole forces. Therefore, the vortex has no orientational effect on the bulk order parameter outside the soft core. In an axial magnetic field, the soft core appears at some critical threshold value of the magnetic field, manifesting a phase transition, where the translational invariance of the $\vec{n}$ vector field is broken. In a tilted field, however, the soft core of the vortex may develop continuously without a phase transition; however, the possibility of a first-order phase transition is not excluded. The soft-core texture may be investigated with the use of ultrasound, whose wavelength is less than the size of the soft core of the vortex. Under such conditions, the additional splitting of the so-called "real squashing mode" (rsq, Ref. 36) should be measured since it yields information about the texture.[37]

Fortunately, the magnetic field $H=284$ G, appropriate to all the presently available experiments with ^{3}He-B vortices, is small enough for one to neglect the soft core, except for a region close to T_c, where due to the experimental difficulties the NMR data on the vortices in ^{3}He-B are not very accurate. Therefore, we may here consider the vortex structure as rigid and without a second core. In this case of the rigid asymptotics, the influence of the system of vortices on the $\vec{n}$-vector texture is very simple, because the $\vec{n}$ vector is uniform everywhere in the vortex lattice and is oriented by the combined actions of F_{DH} and of the vortices. The orientational energy of the vortices arises due to the effect that the magnetic energy in Eq. (6.4) depends on the asymptotics. Indeed, on inserting the axisymmetric *Ansatz* of Eq. (3.14) into Eq. (6.4), and averaging over ϕ, we find the following dependence of the energy density on the orientation of $R_{\alpha i}(\vec{n},\theta)$:

$$\begin{aligned} F_{HV} &= \tfrac{1}{2}(\chi_N-\chi_B)\sum_\nu \left|\sum_\mu H_\alpha R_{\alpha i}\lambda_i^\mu C_{\mu\nu}\right|^2 \\ &= \tfrac{1}{2}(\chi_N-\chi_B)(H_\alpha R_{\alpha i}\hat{z}_i)^2 \\ &\quad\times\sum_\nu(|C_{0\nu}|^2-\tfrac{1}{2}|C_{+\nu}|^2-\tfrac{1}{2}|C_{-\nu}|^2) \\ &\quad+\tfrac{1}{4}(\chi_N-\chi_B)H^2\sum_\nu(|C_{+\nu}|^2+|C_{-\nu}|^2)\,. \end{aligned} \tag{6.8}$$

The orientational part of this energy should be averaged over the vortices which are distributed in a container rotating with the angular velocity Ω with the equilibrium density of vortices given by

$$n_v = \frac{2\Omega}{h/2m_3}\,. \tag{6.9}$$

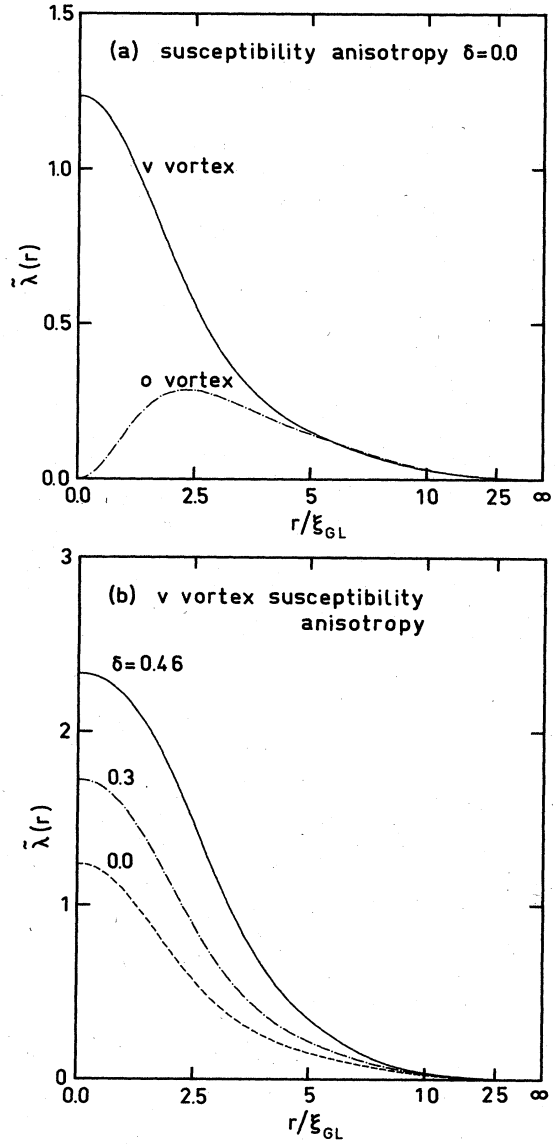

FIG. 15. Radial distributions of the normalized vortex susceptibility anisotropy $\tilde{\lambda}(r)=\sum_\nu[C_{0\nu}^2-\frac{1}{2}(C_{+\nu}^2+C_{-\nu}^2)]$. (a) Comparison of the o vortex [Fig. 3(a)] and the v vortex [Fig. 7(a)] susceptibility anisotropies in the weak-coupling limit ($\delta=0.0$). Because of the normal core structure, $\tilde{\lambda}(r)$ for the o vortex tends to zero on the vortex axis, resulting in a much lower integrated value than for the v vortex. Because of the weak dependence of the o vortex on pressure, $\tilde{\lambda}(r)$ is practically the same for all values of δ. (b) The strong pressure variation of the v vortex (cf. Fig. 7) results in the sensitive pressure dependence of the normalized v vortex susceptibility anisotropy. Note, in particular, the strong increase of the core contribution to $\tilde{\lambda}$ for increasing δ.

This yields the following expression for the density of orientational energy, which proves convenient to write in terms of the dimensionless vortex parameter λ introduced in Ref. 31 for a comparison of the orientational effects of F_{DH} and the vortices:

$$F_v = \tfrac{2}{5}\lambda a (H_\alpha R_{\alpha i}\hat{z}_i)^2 \tag{6.10}$$

with

$$\lambda = \frac{5}{4a}(\chi_N - \chi_B)(2\pi n_v \xi_{\rm GL}^2)\int_0^{R/\xi_{\rm GL}} d\tilde{r}\,\tilde{r}\,\tilde{\lambda}(\tilde{r})\ ,$$
$$\tilde{\lambda} = \sum_\nu (\,|C_{0\nu}|^2 - \tfrac{1}{2}|C_{+\nu}|^2 - \tfrac{1}{2}|C_{-\nu}|^2)\ . \tag{6.11}$$

Here R is the intervortex spacing

$$R = \frac{1}{(\pi n_v)^{1/2}}\ , \tag{6.12}$$

which serves as the cutoff of the logarithmically divergent integral, because the asymptotics of $\tilde{\lambda}$ is given by

$$\tilde{\lambda}(\tilde{r}\to\infty) = \left[1+\frac{3\beta_{12}}{\beta_{345}}\right]\frac{m^2}{\tilde{r}^2}\ , \tag{6.13}$$

where $m=1$ for the singly quantized vortices. This is the effect of the B-phase distortion due to the superflow around the vortex core. The distributions of $\tilde{\lambda}(\tilde{r})$ for the different vortices are shown in Fig. 15. The integral value may be expressed as

$$\int_0^{R/\xi_{\rm GL}} d\tilde{r}\,\tilde{r}\,\tilde{\lambda}(\tilde{r}) = \left[1+\frac{3\beta_{12}}{\beta_{345}}\right]\ln\left[\frac{R}{r_{\rm core}}\right] + b\ , \tag{6.14}$$

where $r_{\rm core}$ is the vortex core radius. The first term in (6.14) may be ascribed to the orientational effect of superflow,[31] while the value b in (6.14) is due to the effect of the magnetic anisotropy inside the vortex core.[33,38] The values of b and $(1+3\beta_{12}/\beta_{345})\ln(R/r_{\rm core})$ for $R=10^{-2}$ cm ($\sim 10^4\xi_{\rm GL}$) for the o and v vortices are collected in Tables II and III for different values of the strong-coupling parameter δ. One may see that the core effect rapidly increases with increasing δ and it is comparable to the effect of the superflow. For example, at the polycritical point ($\delta=0.46$) we find the core contribution near T_c to be $\tilde{\lambda}_{\rm core}=\frac{1}{3}\tilde{\lambda}_{\rm tot}$. However, the flow contribution to $\tilde{\lambda}$ must vanish for $T\to 0$ since it arises from the anisotropy of the superflow, which disappears at low temperatures. Hence only the core contribution $\tilde{\lambda}_{\rm core}$ remains finite at zero temperature, $\tilde{\lambda}_{\rm core}(T=0)=\tilde{\lambda}_{\rm tot}(T=0)$, and the total orientational effect of the vortices is produced at $T=0$ by the susceptibility anisotropy of the vortex core alone.

VII. THE MAGNETIC MOMENT OF THE VORTEX

As is well known by now, the magnetic moment (or nonunitary order parameter) is an intrinsic property of quantized vortices in Fermi superfluids with triplet pairing.[8] It was first predicted for the vortices in a $^3P_2$ paired superfluid state, which may exist inside neutron stars[12] and was experimentally discovered in ^{3}He-B.[3] This magnetic moment is the result of the specific coupling which occurs between the spin and orbital motions of the Cooper pairs, caused by the peculiar breaking of the relative spin-orbital symmetry. The circulation of the superflow around the vortex axis produces an internal orbital rotation of the pairs, which in turn produces the net spin of the pairs due to this spin-orbital coupling.

Here we calculate the magnetic moment for the o and v vortices. In the Ginzburg-Landau regime, the intrinsic magnetic moment density of the superfluid ^{3}He is

$$M_\alpha = \tfrac{1}{3}\gamma N(0)\frac{\eta}{T_c} ie_{\alpha\beta\gamma} A_{\beta i} A^*_{\gamma i}\ . \tag{7.1}$$

The above parameter η is not well known theoretically because it depends on the details of the particle-hole asymmetry near the ^{3}He Fermi surface. Experimentally, it may be estimated from the thermodynamics of the second-order transition occurring in high magnetic fields, where the magnetically ordered A_1 phase appears. In the Ginzburg-Landau functional,[39] the thermodynamics of this transition is governed by a term which is linear in the magnetic field:

$$F_M = -\vec{M}\cdot\vec{H}\ . \tag{7.2}$$

At the melting pressure, η is estimated[40] to equal 0.05.

For the bulk B phase $M_\alpha=0$; however, for the vortex $\vec{M}\neq\vec{0}$, due to the distortion of the B phase in the vortex core. Substituting in Eq. (7.1) the axisymmetric order parameter (3.14) and averaging over the azimuthal angle ϕ, one obtains the following dependence of the intrinsic magnetic moment on the distance from the vortex core:

$$M_\alpha(r) = R_{\alpha i}\hat{z}_i m_0 \sum_\nu (\,|C_{+\nu}|^2 - |C_{-\nu}|^2)\ , \tag{7.3}$$

where

$$m_0 = \tfrac{1}{3}\gamma N(0)\eta\frac{\Delta^2}{T_c}\ . \tag{7.4}$$

Note that the direction of the magnetic moment is fixed by the asymptotics of the order parameter: $M_\alpha \sim R_{\alpha i}\hat{z}_i$. This is the result of the broken relative spin-orbital symmetry, due to which the magnetic moment direction and the direction of the orbital angular momentum (in this case it is the angular momentum of the superflow around the vortex axis, which is directed along $\vec{\Omega}$) are coupled via the order-parameter matrix $R_{\alpha i}$.[41,42] There is no additional symmetry constraint on the expression $\sum_\nu(|C_{+\nu}|^2 - |C_{-\nu}|^2)$; therefore, the net magnetization is nonvanishing for each of the vortices. The distribution of the magnetization for the different vortices are shown in Fig. 16.

The magnetic moment of the vortices was observed[3] due to its specific influence on the NMR signal, which depends on the direction of rotation: The energy in Eq. (7.2) produces an orientational effect on the order parameter $R_{\alpha i}(\vec{n},\theta_0)$, which changes its sign when the direction of magnetic field (or rotation) is reversed. The corresponding orientational gyromagnetic energy, which is linear in $\vec{H}$ and $\vec{\Omega}$, is obtained by averaging (7.2) and (7.3) over the vortices, which are assumed to have the equilibrium density n_v:

$$F_{\rm gm} = \tfrac{4}{5}a\kappa(H_\alpha R_{\alpha i}\hat{\Omega}_i)\ , \tag{7.5}$$

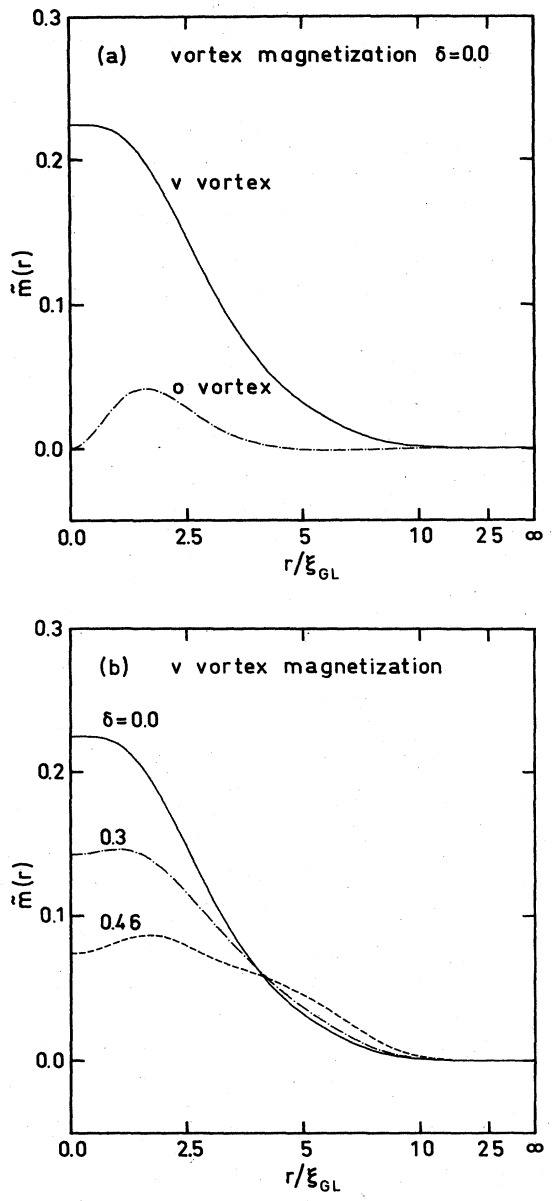

FIG. 16. Normalized magnetization density $\tilde{m}(r) = \sum_\nu (C^2_{+\nu} - C^2_{-\nu})$. (a) For the o and v vortices in ^{3}He-B in the weak-coupling limit. The large value of the v vortex magnetization is essentially due to the distribution of the spontaneously ferromagnetic β phase in the core. The vanishing of the o vortex magnetization on the vortex axis is due to the normal core. (b) The distribution of the v vortex magnetization as a function of the strong-coupling parameter δ. For $\delta=0.0$ the ferromagnetic β phase peaks on the vortex axis [cf. Fig. 7(a)]; this leads to the large value of $\tilde{m}(r=0)$. For increasing δ the value of the intercept $C_{+0}(r=0)$ in Fig. 7 decreases. This leads also to the decrease in the magnetization at the vortex axis. However, the extent of the β phase grows simultaneously and leads to the broader distribution of the vortex magnetization, resulting in roughly the same integrated value for $\tilde{m}$ (cf. Table III). For $\delta=0.46$ the rapid increase of another ferromagnetic phase, the A_1 phase [C_{++}, cf. Fig. 7(c)], associated with the above-described behavior of the β phase, accounts for the features seen in this figure.

where

$$\kappa = -\frac{5}{4a} m_0 (2\pi \xi^2_{GL} n_v) \int_0^\infty d\tilde{r}\,\tilde{r} \sum_\nu (|C_{+\nu}|^2 - |C_{-\nu}|^2) . \tag{7.6}$$

Here again the parameter a is introduced to compare the gyromagnetic energy with the other orientating effects F_{DH} [Eq. (6.5)] and F_v [Eq. (6.10)]. Here, instead of $\hat{z}$, the unit vector $\hat{\Omega}$ along $\vec{\Omega}$ is introduced: The vortex axis $\hat{z}$ is directed along the angular velocity vector $\vec{\Omega}$ and it changes sign with the reversal of rotation due to the change of the circulation quantum number m to the opposite, such that $\hat{z}=\hat{\Omega}$. The values of the integral in (7.6) are shown in Tables II and III for the different vortices and for different values of the strong-coupling parameter δ.

For a rough estimation of the order of magnitude of κ, let us take the following values for the parameters involved [all the parameters, except η, are taken at the pressure $p=18$ bars (Refs. 11 and 40)]:

$$\begin{aligned} &\gamma = -2\times 10^4\ \mathrm{G^{-1}\,sec^{-1}}\ , \quad \eta = 0.05\ , \\ &n_v = 0.3\times 10^4\ \mathrm{cm^{-2}}\ \ (\text{at } \Omega = 1\ \text{rad/sec})\ , \\ &\Delta^2 = 10^{-36}(1-T/T_c)\ \mathrm{erg^2}\ , \\ &N(0) = 10^{38}\ \mathrm{erg^{-1}\,cm^{-3}}\ , \\ &\xi^2_{GL} = 1.6\times 10^{-12}(1-T/T_c)^{-1}\ \mathrm{cm^2}\ , \\ &a = 10^{-12}\ , \quad T_c = 3.2\times 10^{-19}\ \mathrm{erg}\ , \end{aligned} \tag{7.7}$$

and then

$$\kappa \sim (4\ \mathrm{G}) \int_0^\infty d\tilde{r}\,\tilde{r} (|C_{+\nu}|^2 - |C_{-\nu}|^2) . \tag{7.8}$$

This is in agreement with the experimental data[3] on κ,[3] within the order of magnitude. However, the detailed comparison is quite difficult, due to the poorly known value of the parameter η and also because the more reliable experimental data for κ is obtainable only far from T_c. The experimental data for κ at $p=18$ bars and low temperatures $0.5 < T/T_c < 0.7$ may be written as[43]

$$\kappa(\Omega = 1\ \text{rad/sec}) \sim (50\ \mathrm{G})(0.8 - T/T_c)\ , \tag{7.9}$$

which is in quite reasonable agreement with the magnitude of the vortex magnetization [Eq. (7.8) and Table III] calculated in the present paper for the v vortex.

VIII. PHYSICAL PROPERTIES OF VORTICES WITH BROKEN PARITY

One of the most interesting phenomena which occur when parity P is broken is the appearance of a spontaneous electric polarization of the vortex.[44] Here we consider this effect and other consequences of parity violation. We are interested in physical properties that are invariant under gauge transformation and spin rotations, such as electric polarization $\vec{P}$ and supercurrent $\vec{j}_s$. For them, all the elements of these transformations are trivial, and we have the following simplification for the discrete symmetry elements P_1, P_2, and P_3:

$$P_1=P\ ,\quad P_2=PTU_2\ ,\quad P_3=TU_2\ , \tag{8.1}$$

with U_2 denoting an orbital rotation through π around an axis perpendicular to the vortex.

Let us consider the symmetry of the projection of the electric dipole moment $\vec{d}$ of the vortex on the vortex axis $\hat{\Omega}$. This quantity, $\vec{d}\cdot\hat{\Omega}$, has the following parity properties under the transformations given in Eq. (8.1):

$$P_1\vec{d}\cdot\hat{\Omega}=-\vec{d}\cdot\hat{\Omega}\ ,\quad P_2\vec{d}\cdot\hat{\Omega}=\vec{d}\cdot\hat{\Omega}\ ,\quad P_3\vec{d}\cdot\hat{\Omega}=-\vec{d}\cdot\hat{\Omega}\ . \tag{8.2}$$

This is just the symmetry property of the variable v in Eq. (3.23b). Since $\vec{d}\cdot\hat{\Omega}$ changes sign in the P_1 and P_3 transformations, it should vanish for those vortices where these symmetries are conserved. Therefore, the spontaneous electric dipole moment may arise only when the symmetries P_1 and P_3 are broken, and the variables represented as v appear. This is just the case for the v (cf. Fig. 7) and uvw vortices in the B phase, and for the Anderson-Toulouse-Chechetkin vortex texture in the A phase of superfluid ^{3}He, which according to its symmetries is also a P_2 symmetric v vortex.[44]

Let us first consider the electric polarization in this A-phase vortex. The Anderson-Toulouse-Chechetkin vortex texture has the following form in terms of superflow $\vec{v}_s$ and the orbital anisotropy vector $\vec{l}$:

$$\vec{l}=\hat{z}\sin[\eta(r)]\pm\hat{r}\cos[\eta(r)]\ ,$$
$$\vec{v}_s=\frac{\hbar}{2m_3 r}\{1-\sin[\eta(r)]\}\hat{\phi}\ . \tag{8.3}$$

This is a continuous axisymmetric $m=2$ vortex texture. For a detailed discussion of the symmetry classification of the axisymmetric A-phase vortices, see Refs. 15 and 17. The signs $\pm$ above indicate the degeneracy of the v vortex, η changes from $\pi/2$ at the vortex axis to $-\pi/2$ outside the vortex core region. The difference in the physical properties of these two degenerate states is described below. The polarization $\vec{P}(\vec{r})$ in the A phase arises due to the so-called flexoelectric effect, which is well known for ordinary (nonsuperfluid) liquid crystals,[45] where the electric polarization is caused by the bending of the anisotropy axes.

In the A phase there are three flexoelectric parameters, relating $\vec{P}(\vec{r})$ with the gradients of the order parameter:

$$\vec{P}(\vec{r})=\beta_1\vec{l}(\vec{\nabla}\cdot\vec{l})+\beta_2\frac{m_3}{\hbar}\vec{l}\times(\vec{v}_s-\vec{v}_n)+\beta_3(\vec{l}\cdot\vec{\nabla})\vec{l}\ . \tag{8.4}$$

These parameters β_i were estimated[44] to be

$$\beta_1-\beta_3\sim\beta_2\sim(10^{-10}-10^{-9})(1-T/T_c)^2\ \text{V}\ , \tag{8.5a}$$
$$\beta_1+\beta_3\sim10^{-7}(1-T/T_c)\ \text{V}\ . \tag{8.5b}$$

Integrating $\vec{P}(\vec{r})$ in Eq. (8.4) over the cross section of the twofold degenerate Anderson-Toulouse-Chechetkin vortices (8.3), we obtain the dipole moment $\vec{d}$ per unit length of the vortex line:

$$\vec{d}=\pm\hat{\Omega}\left[2\pi\int_0^\infty dr\left[\tfrac{1}{2}\beta_2\cos\eta(1-\sin\eta)+(\beta_3-\beta_1)r\frac{\partial\eta}{\partial r}\cos^2\eta\right]\right]\ . \tag{8.6}$$

The magnitude of $\vec{d}$ is the same for both vortices and it is proportional to the radius r_{core} of the vortex core. However, they have the opposite senses for the direction of the electric dipole moment along the vortex axis, which reflects the degeneracy resulting from the broken P symmetry. Note that only the parameters β_2 and $\beta_1-\beta_3$ are involved in the dipole moment $\vec{d}$ in Eq. (8.6), because the parameter $\beta_1+\beta_3$ is a prefactor of the term in Eq. (8.4), which is a pure derivative, and therefore cannot contribute to the total dipole moment of the vortex.

The same effect of spontaneous polarization also takes place for the v and uvw vortices in ^{3}He-B. The quantity $\vec{d}$ is here proportional to the core radius of these vortices, which is $\sim\xi_{\text{GL}}$. The estimation of $\vec{d}$ may be carried out readily on recalling that the cores of these vortices predominantly consist of the A phase; therefore, the same parameters β_i as in Eq. (8.4) are involved:

$$\vec{d}\sim\pm\hat{\Omega}(\beta_1-\beta_3)\xi_{\text{GL}}\ . \tag{8.7}$$

The twofold degeneracy of the v vortex gives rise to topologically stable kinks or point solitons separating two parts of the vortex line with different electric polarizations. Such a point on the vortex line has an electric charge e^* associated with it, which is of the order of

$$e^*\sim(\beta_1-\beta_3)\xi\sim10^{-7}e\ , \tag{8.8}$$

for the vortex line in the B phase. In the above, e denotes the elementary charge of an electron.

For the A-phase vortex in an applied magnetic field, where the core radius r_{core} is of the order of the dipole length $\xi_D\sim10^{-3}$ cm, the corresponding electric charge associated with a point soliton is of the order of

$$e^*\sim(\beta_1-\beta_3)\xi_D\sim10^{-5}e\ . \tag{8.9}$$

An equal amount of electric charge ought to be concentrated on the endpoint of the vortex line at the surface of the container.

Under ordinary circumstances, the signs of these charges at the surface are randomly disordered, due to the disorder in the sense of the direction of the vortex polarization, $\vec{d}\sim\pm\hat{\Omega}$. Thus the bulk liquid has no features of the broken symmetry. However, the situation will be different if a strong orientating electric field is applied for a period of time along the axis of rotation. In this case, there will result a surplus of vortices with their polarization $\vec{d}$ along the electric field, and the bulk liquid ^{3}He will acquire features of the broken symmetry. This is exactly analogous to a liquid crystal containing chiral molecules with broken parity, which corresponds to the v vortices in rotating superfluid ^{3}He. If the signs of chirality of these molecules are disordered, this is an ordinary nematic liquid crystal. But if there is a surplus of molecules with a given sign of chirality, then the parity in the liquid crys-

tal is violated, and it becomes a cholesteric liquid crystal. Due to the parity violation, the free energy of the cholesteric contains an additional term, which is linear in the gradient of the order parameter; this produces the helicity in the order-parameter distribution.

Essentially the same phenomena will occur in rotating superfluid ^{3}He, if there is a surplus of vortices with a given electric polarization, produced, for example, by turning on an external electric field for a period of time. In the B phase these vortices will produce terms, in addition to those in Eqs. (6.10) and (7.5) in the macroscopic free energy (i.e., on a length scale larger than the intervortex spacing), which are linear in the gradient of the order parameter $R_{\alpha i}$, which is a slow variable on the intervortex distance. They may be extracted from the ordinary quadratic terms in the gradient expansion in Eq. (4.4) if one inserts the order parameter

$$A_{\alpha i}=R_{\alpha j}(\vec{r})A^0_{ji}(\vec{r}) \tag{8.10}$$

into this Eq. (4.4). Here $A^0_{ji}(\vec{r})$ denotes the order parameter in the vortex core texture with the asymptotics $A^0_{ji}=\Delta\delta_{ji}$ far from the vortex core, and $R_{\alpha j}$ is the slow variable of the macroscopic texture, as in Eqs. (6.10) and (7.5). Inserting Eq. (8.10), for example, into the second term of the gradient energy in Eq. (4.4), one obtains the following term, which is linear in the gradient of $R_{\alpha i}$:

$$F_{\rm lin}=K_2R_{\alpha p}\partial_iR_{\alpha q}(A^0_{qi}\nabla_j A^{0*}_{pj}+A^{0*}_{qi}\nabla_j A^0_{pj}) . \tag{8.11}$$

The last part of this equation, which is nonzero only in the vortex core, may be integrated over the cross-sectional area of the vortex core. If the vortices are identical, this yields

$$F_{\rm lin}=n_VK_2R_{\alpha p}\partial_iR_{\alpha q}\int dS(A^0_{qi}\nabla_j A^{0*}_{pj}+A^{0*}_{qi}\nabla_j A^0_{pj}) . \tag{8.12}$$

The integral is nonvanishing for the v and uvw vortices, and its part, which produces nonzero Eq. (8.12), equals

$$K_2\int dS(A^0_{qi}\nabla_j A^{0*}_{pj}+A^{0*}_{qi}\nabla_j A^0_{pj})=\epsilon(\delta_{qi}\hat{z}_p-\delta_{pi}\hat{z}_q) , \tag{8.13}$$

where the parameter ϵ is of the order of $\rho_s\xi_{\rm GL}(\hbar/m_3)^2$.

If the vortices are not identical, then Eq. (8.12) should be multiplied by the fraction η of the relative surplus of the vortices with the electric polarization in the $\hat{z}$ direction. Hence, $\eta=0$ for randomly disordered electric polarizations (or for vortices with zero polarization), while $\eta=1$ for the fully saturated polarization. Equations (8.12) and (8.13) produce an additional orientating effect on the order-parameter texture in the rotating B phase, which is due to the presence of vortices. Hence the NMR signal should change after turning on the external electric field for a period of time necessary to result in an ordered polarization of the vortices, if there are v or uvw vortices in the rotating ^{3}He-B.

Note that if the vortices are polarized, there occurs a nonvanishing surface density of electric charge ηe^*n_V, which results in a spontaneous electric field in the rotating bulk liquid ^{3}He, which is given by $4\pi\eta e^*n_V$.

Let us now consider the symmetry of the superflow along the vortex axis, $\vec{j}_s\cdot\hat{\Omega}$. Under the symmetry transformations, this quantity changes as the variable w in Eq. (3.23c):

$$P_1\vec{j}_s\cdot\hat{\Omega}=-\vec{j}_s\cdot\hat{\Omega} , \quad P_2\vec{j}_s\cdot\hat{\Omega}=-\vec{j}_s\cdot\hat{\Omega} , \quad P_3\vec{j}_s\cdot\hat{\Omega}=\vec{j}_s\cdot\hat{\Omega} . \tag{8.14}$$

This implies that a spontaneous superflow arises in the cores of the w and the uvw vortices. The superfluid current along the vortex axis in the ^{3}He-B vortex is of the order of

$$j_s\sim\pm\hat{\Omega}\rho_s\frac{\hbar}{m_3}\xi_{\rm GL} . \tag{8.15}$$

Just as for the electric dipole moments of the v and uvw vortices, the axial supercurrents in the w and uvw vortices may be ordered or disordered. The ordering may be produced by an external superflow applied along the axis of rotation.

The superflow along the vortex axis could be observed with ultrasound applied along the vortex axis: For a randomly disordered superflow array, there should occur a Doppler splitting of the ultrasound absorption, while in the case of fully aligned superflow, only a single Doppler-shifted ultrasound absorption spectrum should be observed.

A spontaneous superflow may also exist in the A-phase vortices. The real vortices in the NMR experiments are not axially symmetric. However, they do possess the same elements of discrete symmetry and hence a similar symmetry classification. Numerical calculations showed[5] that there are two possible candidates for the observed vortex: the v vortex and the w vortex. Both have similar magnetic properties. However, the w vortex possesses a spontaneous superflow, which is 3 orders of magnitude larger than that for the B-phase w vortex, while the electric polarization of the v vortex is also 3 orders of magnitude larger than that for the B-phase v vortex. This follows essentially from the fact that the core radius of the continuous A-phase vortices is larger by a factor of 10^3 than the radius $r_{\rm core}$ of the B-phase vortices.

IX. DISCUSSION

We have presented the classification of the possible axially symmetric vortices in superfluid ^{3}He. Using this classification, we have constructed the Landau theory of the phase transitions inside the vortex core matter of the ^{3}He-B vortices. It is possible that the observed first-order phase transition in the vortex core structure is determined by this theory. However, the complete identification of the vortices that have been observed in the NMR experiments in terms of our classification scheme is not possible at present, especially because all the numerical calculations of the vortex core structures and of their mutual stability were carried out in the Ginzburg-Landau regime near T_c. Therefore, it is most important to find out experimentally whether or not the vortex phase transition line actually tends to T_c. Near T_c, we have found only

one stable vortex core structure—the v vortex—in which one of the discrete vortex symmetries is broken, and which displays a superfluid core structure with A phase accompanied with the spontaneously ferromagnetic β phase.

Recently Passvogel, Tewordt, and Schopohl[46] have repeated our numerical calculations of the structures of the o, u, v, w, and uvw vortices which were first reported in Ref. 8 and they have reconfirmed our previous result that the v vortex is the stable one among the singly quantized axisymmetric vortices in superfluid ^{3}He-B for all pressures in the Ginzburg-Landau regime. However, Fetter and Theodorakis[47] have argued that there should be a transition from the v vortex at low pressures to the o vortex at high pressures. This is contrary to our results, reproduced by Passvogel, Tewordt, and Schopohl.[46] Our calculations (and also those in Ref. 46) are based on a full numerical minimization of the vortex energy functional. This is vital, since the vortex energies are sensitive to any numerical inaccuracies. At present it is not yet clear whether the phase transition that Fetter and Theodorakis suggest is only due to (i) the extremely rough numerical scheme that they employ to approximately describe the vortex structures (for which full minimizations already exist) such that the approach of Fetter and Theodorakis apparently loses any quantitative predictive power, or whether it is due to (ii) properties of the Sauls-Serene parametrization of the strong-coupling corrections to the β parameters, which yields a phase transition even in bulk ^{3}He from the B phase to the A phase at too low a pressure. Certainly one should not calculate the vortex core structure in the B phase with β values corresponding to stable A phase.

Further arguments suggesting that the results of Fetter and Theodorakis are suspect to be an artifact of either of the above causes are the following. (i) Our phenomenological Landau theory of the phase transitions among the axisymmetric vortices (first presented in Ref. 8 and in detail in Sec. III of the present paper) suggests that the transition from the v vortex to the o vortex should be of second order; therefore, the transition that Fetter and Theodorakis suggest probably has nothing to do with the first-order transition[6,7] seen in the experiments. (ii) Especially, unlike Fetter and Theodorakis, we find that the A-phase amplitude and its extent in the vortex core increases with pressure [see (a)—(c) of Fig. 7 in the present paper], as one should expect on physical grounds since the nucleation of the A phase is preferred at higher pressures also in the bulk superfluid ^{3}He. (We note in passing that ion trapping by the B-phase vortices[48] and the possible consequent measurements of ion mobility along the vortex lines in ^{3}He-B could potentially shed interesting new information on the nature of the pairing state in the core of the high-pressure vortex in the B phase.)

Provided that the vortex phase-transition line in fact does approach T_c, then there should coexist two different stable vortex solutions at the appropriate pressure in the Ginzburg-Landau regime. Therefore, the v vortex should be unstable towards further breaking of symmetry, because in this case several different vortices may appear with the first-order phase transition between them. All of these new vortices in fact have superfluid cores which are magnetic. The investigation of these instabilities requires a lot of numerical efforts, but the expenditure of this computer time will be justified if the vortex transition line will be found to really approach T_c. If the vortex transition does not tend to T_c, then it is possible that far from T_c the v vortex transforms either into the u or the w vortex. Since these have broken symmetries different from that of the v vortex, the $v \rightarrow u$ and the $v \rightarrow w$ transitions may be only of the first order. In this case it will be necessary to investigate the vortex core structure with the use of the Gor'kov equations. However, the information necessary for the vortex identification may be extracted from the qualitative inspection of the vortex phase diagram upon comparing it with the results of the catastrophe theory. This must include the systematic detailed measurement of the catastrophe lines, which may be found from experiments on the vortex metastability phenomena, which have already been partially observed[2] in the course of measurements under continuous rotation.

ACKNOWLEDGMENTS

We are grateful to Yu.M. Bunkov, P. J. Hakonen, O. T. Ikkala, S. T. Islander, M. Krusius, R. E. Packard, J. P. Pekola, and J. T. Simola for useful discussions on the experiments and to A. L. Fetter, I. A. Fomin, G. A. Kharadze, V. P. Mineev, S. P. Novikov, T. Ohmi, L. P. Pitaevskii, J. A. Sauls, N. Schopohl, and A. Veselov for theoretical conversations. In particular, it is our pleasure to thank O. V. Lounasmaa for his stimulating interest in our work and for continual encouragement. This research is supported by the Academy of Finland, the Commission for Scientific and Technical Collaboration between Finland and the Soviet Union, and the U.S.S.R. Academy of Sciences. One of us (M.M.S.) is grateful to the Finnish Cultural Foundation and the Academy of Finland for support.

[1]P. J. Hakonen, O. T. Ikkala, S. T. Islander, O. V. Lounasmaa, and G. E. Volovik, J. Low Temp. Phys. 53, 425 (1983).

[2]Yu.M. Bunkov, P. J. Hakonen, and M. Krusius, in *Quantum Fluids and Solids—1983 (Sanibel Island, Florida)*, proceedings of the Symposium on Quantum Fluids and Solids, edited by E. D. Adams and G. G. Ihas (AIP, New York, 1983), p. 194.

[3]P. J. Hakonen, M. Krusius, M. M. Salomaa, J. T. Simola, Yu.M. Bunkov, V. P. Mineev, and G. E. Volovik, Phys. Rev. Lett. 51, 1362 (1983).

[4]H. K. Seppälä and G. E. Volovik, J. Low Temp. Phys. 51, 279 (1983).

[5]H. K. Seppälä, P. J. Hakonen, M. Krusius, T. Ohmi, M. M. Salomaa, J. T. Simola, and G. E. Volovik, Phys. Rev. Lett. 52, 1802 (1984).

[6]O. T. Ikkala, G. E. Volovik, P. J. Hakonen, Yu.M. Bunkov, S. T. Islander, and G. A. Kharadze, Pis'ma Zh. Eksp. Teor. Fiz. 35, 338 (1982) [JETP Lett. 35, 416 (1982)].

[7]J. P. Pekola, J. T. Simola, P. J. Hakonen, M. Krusius, O. V. Lounasmaa, K. K. Nummila, G. Mamniashvili, R. E. Packard, and G. E. Volovik, Phys. Rev. Lett. 53, 584 (1984).

[8]M. M. Salomaa and G. E. Volovik, Phys. Rev. Lett. **51**, 2040 (1983).
[9]T. Passvogel, N. Schopohl, and L. Tewordt, J. Low Temp. Phys. **50**, 509 (1983).
[10]T. Ohmi, T. Tsuneto, and T. Fujita, Progr. Theor. Phys. **70**, 647 (1983).
[11]S. Theodorakis and A. L. Fetter, J. Low Temp. Phys. **52**, 559 (1983).
[12]See, for example, R. Tamagaki, Progr. Theor. Phys. **44**, 905 (1970); T. Takatsuka and R. Tamagaki, *ibid.* **46**, 114 (1971); R. W. Richardson, Phys. Rev. D **5**, 1883 (1972); J. A. Sauls, D. L. Stein, and J. W. Serene, *ibid.* **25**, 967 (1982), and references therein.
[13]R. Thom, *Structural Stability and Morphogenesis* (Benjamin, New York, 1975); V. I. Arnol'd, A. N. Varzenko, and C. M. Gusein-Zade, *Singularities of Differentiable Mappings* (Nauka, Moscow, 1982).
[14]M. M. Salomaa and G. E. Volovik, Phys. Rev. Lett. **52**, 2008 (1984).
[15]M. M. Salomaa and G. E. Volovik, Helsinki University of Technology, Department of Technical Physics, Report No. TKK-F-A539 (1984) (unpublished).
[16]M. M. Salomaa (unpublished).
[17]M. M. Salomaa and G. E. Volovik (unpublished).
[18]For reviews on the topology of defects in condensed matter, see N. D. Mermin, Rev. Mod. Phys. **51**, 591 (1979); V. P. Mineev, in *Soviet Scientific Reviews, Section A: Physics Reviews,* edited by I. M. Khalatnikov (Harwood, New York, 1980), Vol. 2, p. 173; H.-R. Trebin, Adv. Phys. **31**, 195 (1982); M. Kléman, *Points, Lines and Walls in Liquid Crystals, Magnetic Systems and Various Ordered Media* (Wiley, New York, 1983).
[19]D. Kastler, M. Mebkhout, G. Loupias, and L. Michel, Commun. Math. Phys. **27**, 195 (1972); M. Kléman and L. Michel, Phys. Rev. Lett. **40**, 1387 (1978); L. Michel, Rev. Mod. Phys. **52**, 617 (1980).
[20]R. B. Jones, J. Phys. C **10**, 657 (1977); G. Barton and M. A. Moore, *ibid.* **7**, 4220 (1974).
[21]G. E. Volovik and L. P. Gor'kov, Pis'ma Zh. Eksp. Teor. Fiz. **39**, 550 (1984).
[22]A. A. Balinskii, G. E. Volovik, and E. I. Katz, Zh. Eksp. Teor. Fiz. **87**, 1305 (1984).
[23]A. V. Nikiforov and E. B. Sonin, Zh. Eksp. Teor. Fiz. **85**, 642 (1983) [Sov. Phys.—JETP **58**, 373 (1983)].
[24]G. E. Volovik and V. P. Mineev, Pis'ma Zh. Eksp. Teor. Fiz. **24**, 605 (1976) [JETP Lett. **24**, 561 (1976)].
[25]N. D. Mermin and G. Stare, Phys. Rev. Lett. **30**, 1135 (1973); D. M. Lee and R. C. Richardson, in *The Physics of Liquid and Solid Helium,* edited by K. H. Benneman and J. B. Ketterson (Wiley, New York, 1978), Vol. II, Chap. IV.
[26]P. W. Anderson and W. F. Brinkman, Phys. Rev. Lett. **30**, 1108 (1973); P. W. Anderson and W. F. Brinkman, in *The Helium Liquids (Proceedings of the Fifteenth Scottish Universities Summer School in Physics),* edited by J. G. M. Armitage and I. F. Farquhar (Academic, London, 1975), p. 315.
[27]G. E. Volovik and V. P. Mineev, Zh. Eksp. Teor. Fiz. **83**, 1023 (1982) [Sov. Phys.—JETP **56**, 579 (1982)].
[28]N. D. Mermin, Physica **90B**, 1 (1977); N. D. Mermin, Physics Today **34**(4), 46 (1981), and references therein.
[29]D. Einzel and M. M. Salomaa (unpublished).
[30]D. D. Osheroff, Physica **90B**, 20 (1977).
[31]A. D. Gongadze, G. E. Gurgenishvili, and G. A. Kharadze, Fiz. Nizk. Temp. **7**, 821 (1981) [Sov. J. Low Temp. Phys. **7**, 397 (1981)].
[32]G. E. Volovik, A. D. Gongadze, G. E. Gurgenishvili, M. M. Salomaa, and G. A. Kharadze, Pis'ma Zh. Eksp. Teor. Fiz. **36**, 404 (1982) [JETP Lett. **36**, 489 (1982)].
[33]M. M. Salomaa and G. E. Volovik, in *Quantum Fluids and Solids—1983 (Sanibel Island, Florida),* proceedings of the Symposium on Quantum Fluids and Solids, edited by E. D. Adams and G. G. Ihas (AIP, New York, 1983), p. 210.
[34]M. M. Salomaa (unpublished).
[35]E. B. Sonin, Pis'ma Zh. Eksp. Teor. Fiz. **38**, 11 (1983) [JETP Lett. **38**, 11 (1983)]; J. Low Temp. Phys. **55**, 533 (1984).
[36]B. S. Shivaram, M. W. Meisel, B. K. Sarma, W. P. Halperin, and J. B. Ketterson, Phys. Rev. Lett. **49**, 1646 (1982).
[37]G. E. Volovik, Pis'ma Zh. Eksp. Teor. Fiz. **39**, 304 (1984).
[38]P. J. Hakonen and G. E. Volovik, J. Phys. C **15**, L1277 (1982).
[39]V. Ambegaokar and N. D. Mermin, Phys. Rev. Lett. **30**, 1981 (1973).
[40]J. C. Wheatley, Rev. Mod. Phys. **47**, 415 (1975).
[41]A. J. Leggett and S. Takagi, Ann. Phys. (N.Y.) **110**, 353 (1978).
[42]G. E. Volovik and V. P. Mineev, Zh. Eksp. Teor. Fiz. **86**, 1667 (1984).
[43]P. J. Hakonen, M. Krusius, and J. T. Simola (private communications).
[44]G. E. Volovik, Pis'ma Zh. Eksp. Teor. Fiz. **39**, 169 (1984).
[45]P. G. de Gennes, *The Physics of Liquid Crystals* (Clarendon, Oxford, 1975).
[46]T. Passvogel, L. Tewordt, and N. Schopohl, J. Low Temp. Phys. **56**, 383 (1984).
[47]A. L. Fetter and S. Theodorakis, Phys. Rev. Lett. **52**, 2007 (1984).
[48]V. P. Mineev and M. M. Salomaa, J. Phys. C **17**, L181 (1984).